**Title:**

# Criteria for the design of tissue-mimicking phantoms for the standardisation of biophotonic instrumentation

**Authors:**

Lina Hacker[1,2], Heidrun Wabnitz[3], Antonio Pifferi[4], T. Joshua Pfefer[5], Brian W. Pogue[6], and Sarah E. Bohndiek[1,2*]

**Affiliations:**

[1] Department of Physics, University of Cambridge, JJ Thomson Avenue, Cambridge, CB3 0HE, U.K.

[2] Cancer Research UK Cambridge Institute, University of Cambridge, Robinson Way, Cambridge, CB2 0RE, U.K.

[3] Physikalisch-Technische Bundesanstalt (PTB), Abbestraße 2-12, 10587 Berlin, Germany

[4] Department of Physics, Politecnico di Milano, Piazza Leonardo da Vinci 32, Milano, Italy

[5] US Food and Drug Administration, Silver Spring, Maryland, USA

[6] Thayer School of Engineering, Dartmouth, Hanover, New Hampshire, USA

**Corresponding author**:

*Sarah E. Bohndiek seb53@cam.ac.uk

## Abstract

The reliability and reproducibility of experimental results are crucial in the development and regulatory approval of medical technologies, yet represent a challenge for biophotonic instrumentation due to a lack of accepted standards and phantoms suitable for successful technical validations. Here, we discuss the general design considerations for the preparation of tissue-mimicking biophotonic phantoms and then critically review the existing literature on phantom materials and fabrication across the field in light of these criteria and of recent developments at the state-of-the-art. We then focus on three representative examples of biophotonic standardisation related to different modalities, presented in order of their relative maturity: diffuse optical imaging and spectroscopy, fluorescence guided surgery, and photoacoustic imaging. Finally, we provide a perspective on future phantom development and the unmet needs of the biophotonic field, identifying a set of criteria, termed the “4Cs”, for biophotonic standardisation which highlight the need for characterisation, collaboration, communication and commitment to maximise the achievements of ongoing standardisation efforts.

Optical imaging biomarkers enable disease diagnosis and treatment in real-time at relatively low cost, leading to an increase in the use of optical imaging methods in clinical practice[1]. Despite the increasing number of available optical-imaging biomarkers and their significant potential for improving clinical outcomes, published standards for performance evaluation of optical imaging devices are still lacking[2]. As a result, technological progress in the respective imaging communities is hampered by a lack of transparency and comparability between system performance evaluations reported in the literature. The lack of consensus standards alsoimpacts the clinical translation process because regulatory bodies often recognize such standards and/or use them to guide policy. Without technical guidance on performance testing, the execution of clinical studies and the approval of new biophotonic devices may be slower and inconsistent.

Test objects to calibrate optical systems have an important subset known as tissue-mimicking phantoms, which are used for performance evaluation of a given technology by mimicking light-tissue interactions of human tissue, as well as other crucial elements of the process[3,4]. The diverse landscape of biophotonic applications means that it is likely impossible to have an all-encompassing phantom that fulfils the needs of every optical sub-speciality. As such, a wide range of biophotonic phantoms have been proposed[5,6], but there has been no consensus on a widely applicable material type nor fabrication method to produce such phantoms. Nevertheless, finding consensus on broadly applicable materials would be beneficial to enable comparison of devices between vendors and institutions; advance hybrid modalities; allow complementary use of different modalities within one clinical session; and further the development of internationally-recognised standards[7,8].

Here, we survey the current state-of-the-art in phantom materials and standardisation efforts in biophotonics.we outline phantom design considerations highlighting important base requirements for an ideal biophotonic phantom. We then discuss phantom materials and their methods of preparation, emphasizing individual strengths and weaknesses in the context of standardisation efforts. We present three examples relevant to current clinical translational efforts: (i) diffuse optical imaging and spectroscopy, (ii) fluorescence guided surgery (FGS), and (iii) photoacoustic imaging (PAI), each showcasing the modality-specific versatility of phantom designs and standardisation approaches. Learning from these prior efforts, recommendations are formulated on how to overcome challenges on the path towards standardisation. We believe that early definition of phantom-based standards will help accelerate clinical translation of biophotonic technologies.

## Biophotonic phantom design considerations

Biophotonic phantoms can be broadly divided into physical phantoms and numerical (computational) phantoms[9]. Numerical phantoms cover *in silico* frameworks, which will not be

reviewed here; physical phantoms are material objects that can be artificially composed or tissue derived. Artificially composed phantoms can be homogenously, heterogeneously or anthropomorphically designed. Tissue-derived phantoms include both *ex vivo* and bioengineered tissues.

## Physical properties of soft tissues

Understanding the physical properties of soft tissues is a fundamental requirement for development, application and evaluation of biophotonic phantoms. Average values for the optical[10,11], acoustic[12,13] and thermoelastic[14] properties of soft tissues are summarised in Supplementary Table 1. To understand light propagation in turbid media, knowledge of the probability of a scattering or absorption event per unit path length is essential. These parameters are captured by the linear scattering coefficient $\mu_s(\lambda)$ and the linear absorption coefficient $\mu_a(\lambda)$; the refractive index n is also relevant for light reflection and refraction at interfaces. For certain microscopic or mesoscopic applications, or interactions near a light source, knowledge of the anisotropy factor g of the phantom medium is important as well. After several scattering events, light transport is diffuse and scattering can be assumed to be isotropic. In these regimes, the reduced scattering coefficient $\mu_s'(\lambda)$ (defined by $\mu_s'(\lambda) = (1\text{-}g)\ \mu_s(\lambda)$) is sufficient to describe the apparent scattering coefficient under the assumption of source to measurement distance >> $1/\ \mu_s(\lambda)$.

Both scattering and absorption effects are wavelength-dependent and determined by the constituents of the medium. In the visible wavelength range in soft tissues, oxyhaemoglobin ($O_2Hb$) and deoxyhaemoglobin (HHb) as well as melanin are the main endogenous chromophores. Moving towards near infrared (NIR) wavelengths (800–2500nm), water, lipids and proteins (mostly collagen) become increasingly absorbent as well. In order to measure optical properties, a wide range of methods can be employed such as spectrophotometers, double-integrating sphere systems, spatial frequency domain imaging and multi-distance frequency domain photon migration techniques as well as time-domain photon migration techniques[15–17]. Yet, the accurate assessment of optical properties of a turbid medium is highly challenging due to the strong absorption-to-scattering coupling for light attenuation and different limitations of the analysis models. Multi-laboratory studies of a liquid phantom showed an agreement within 2% of the estimate for both $\mu_a$ and $\mu_s'$[18], but discrepancies for solid phantoms are commonly found to up to ±15%[19].

For phantoms mimicking acoustic properties, relevant for hybrid biophotonic methodologies such as PAI, it is important to assess how fast an acoustic wave can propagate within a medium and how strongly the medium attenuates the wave. This is captured by the

material-specific speed of sound c and acoustic attenuation coefficient α, respectively. The extent of backscattering is determined by the backscattering coefficient $\mu_{bs,}$ which is difficult to determine and therefore rarely reported[20]. A well-characterized broadband frequency description of these parameters is essential.

For phantoms mimicking tissue fluorescence, the fluorophore absorption coefficient, $\mu_{af}(\lambda)$, and emission spectrum, $I_e(\lambda)$, should ideally match those present in tissue; the emission quantum yield, $\phi_{QY}$, and emission lifetime, $\tau$, could also be matched to the fluorophore of interest if desired. The stability of biological fluorophores, however, is generally poor, meaning degradation of the emission intensity over time is common from light exposure (photobleaching) or from chemical/environmental effects, hence these are rarely used directly in a phantom context.

## The role of phantoms in the translational research pipeline

Phantoms play a fundamental role in standardisation and clinical translation of new devices[3]. In the context of this review, standardisation refers to the process of establishing documentary consensus on a specific technical modality/task outlining precise guidelines, specifications and relevant definitions[21]. While different definitions of the translational pipeline exist[22], most approaches agree that translational research includes those efforts that transform scientific discoveries into novel tools that are actively applied in clinical practice. Along this (not always strictly linear) path, phantoms fulfil a range of tasks that can be roughly divided into instrument-specific (e.g., device development, validation and surveillance) and application-specific tasks (e.g., testing or validation of an anticipated physical measurement; replacement of *in vivo* models) (Fig. 1).

One of the more challenging phases of device translation is often the medical device regulatory process. This process can be streamlined to some degree through implementation of phantom-based test methods, where available, as illustrated using the following examples from the United States (US). An early step in the path to marketing a medical device according to US Food and Drug Administration procedures is often a clinical study approval, or Investigational Device Exemption (IDE). In an IDE application, non-clinical performance testing methods such as phantoms can be implemented to generate data that supports "an expectation of acceptable clinical use[23] and that the device will function as intended." When using a non-standard method, however, it may be necessary to provide adequate justification of the ability of a phantom approach to predict clinical performance. In applications for regulatory clearance of relatively low risk devices through the Premarket Notification, or 510(k) pathway, the need to establish "substantial equivalence" with a predicate device is critical. This can often be accomplished in part through the use of phantom-based test methods[24], which

may involve, for example, characterizing image quality with phantoms and test targets. For higher risk devices that require a Premarket Approval (PMA) submission, clinical data is typically paramount, but phantoms can play a secondary role in establishing effectiveness under well controlled, yet biologically-relevant conditions. Also, PMA supplements that request approval for device modifications can include phantom results. To ensure that test methods are effective in supporting the aforementioned types of regulatory submissions, it is important that they adhere to technical design specifications suitable for the biological scenario under consideration.

### Phantom design properties

An ideal biophotonic phantom material, which intends to cover all outlined tasks, should possess eight important properties (Fig. 2). Usually, however, phantoms are targeted to specific applications, such as the assessment of precision or accuracy. Precision phantoms are focussed on instrument-specific tasks, for example, evaluating repeatability (same subject, same scanner, same operator, short interval) and reproducibility (comparable subjects, different scanner make/model, centres). These can add value in multi-centre clinical trials by providing a common calibration of all instruments across sites[25,26]. For this purpose, temporal and mechanical stability as well as reproducible fabrication are key requirements. For accuracy phantoms, tissue-mimicking properties are of utmost importance, as they aim to faithfully recapitulate the expected signal, which can be either static (replicating a tissue type) or dynamic (replicating a physiological process). Accuracy phantoms are adapted to tissue type, pathology and species (e.g., with differing skin pigmentation, model organism) of interest and can be complex, representing, for example, different layers present in tissue as well as the different chromophores and fluorophores that contribute to the overall optical behaviour of the tissue or pathology. They are most often used for clinical training and testing purposes, or to validate physical models or simulations. In contrast, precision phantoms are employed to evaluate basic device performance metrics, such as signal stability, signal-to-noise, contrast, or resolution, and therefore, only require simpler geometries[27]. Devices that generate quantitative outputs (e.g., blood oxygenation) may require approaches for determining additional metrics such as precision, bias, linearity and sensitivity.

The distinction between these two phantom types is necessary as the final application of the phantom dictates its design and composition.

## Materials and methods for preparation of biophotonic phantoms

Materials for optical phantoms can be broadly divided into water-based and non-water-based materials (Supplementary Table 2), with respective additives used to tune optical and acoustic

properties (Table 1 and 2). The key features that are typically considered when comparing different materials are their tissue-mimicking capabilities and the ease of handling and fabrication (summarised in Table 3), which together with the intended phantom type, determine the overall design and suitability for use in a given application (Supplementary Table 3).

**Tuning of optical and acoustic properties**

The molecular composition of a material type determines its intrinsic properties and the types of additives that can be used to tune such properties. Nevertheless, similar classes of additives have been used in water (Table 1) and non-water based (Table 2) materials to tune optical and acoustic properties[5].

Additives that adjust optical scattering can be broadly classed into (i) lipids, (ii) white metal oxide suspensions, (iii) polymer microspheres and, more rarely, (iv) gold nanoparticles. Lipid-based emulsions such as milk or intralipid are popular in water-based phantoms due to their simple application and biological similarity to fat-based structures found in tissue, allowing incorporation of aqueous absorbers or fluorophores. Here, Intralipid[28,29] (or similar compounds[30] such as Nutrilipid, Lyposyn, Vasolipid, Lipofundin etc), a suspension of soybean oil, egg phospholipids, and glycerol in water, is most commonly employed due to its high stability, low absorption coefficient, regulatory controlled low batch-to-batch variability[30,31] and extensive validation in the literature[18,28–33]. Microspheres are a favourable option for precision phantoms due to their well-controlled size, refractive index and predictable scattering properties in Mie theory[34], but they are typically high cost, limiting their use to small volumes. Metal oxide powders are cost-effective, highly industry produced for all white pigmented materials such as paint, and commonly used in non-water-based phantoms. However, thorough mixing and/or sonication needs to be employed to create homogeneous, repeatable materials without sedimentation or clustering. Titanium dioxide ($TiO_2$) has been a preferred choice due to its negligible NIR absorption and high refractive index[35], but metal oxides with different particle sizes[36] and refractive indices (e.g., aluminium oxide ($Al_2O_3$)[37] or zinc oxide (ZiO)[38,39]) have been used as well. Gold nanoparticles[40] have been also employed as a scattering agent[41], but they are relatively high in cost and also exhibit optical absorption.

To adjust optical absorption, either natural tissue chromophores (e.g., haemoglobin or melanin) or synthetic absorbers (e.g., pigment-based inks, molecular dyes, etc.) can be used[5]. The biological chromophores are able to provide absorption spectra similar to soft tissue, but are often unstable and restricted to use in aqueous environments[5]. Synthetic absorbers can exhibit both flat (e.g., India ink[42,43]) or peaked (e.g., Naphthol Green[44], Trypan Blue[45]) absorption spectra, but with higher stability. Care must be taken when employing molecular dyes in water-based phantoms, as diffusion and degradation processes can occur[42]. Also,

subtle fluorescence emission can produce strong artefacts in turbid materials due to long photon pathlengths increasing fluorescence contamination. In contrast to molecular dyes, pigment-based inks consist of larger particles and cannot diffuse through a gel or polymer-matrix, but their optical absorption is often accompanied by additional scattering[43]. India ink, a suspension of insoluble carbon particles in aqueous medium, is one of the most popular options as the ink is chemically and spectroscopically stable, non-toxic, non-fluorescent and offers a flat absorption spectrum with little variation over the visible and NIR region[42,43]. In general, absorbers need to be chosen carefully with regard to the base material as solubility may be limited and hardening of the base material can impact the absorption properties[46].

The acoustic properties of a material are closely connected to its mechanical composition and are, therefore, more difficult to tune with external agents. In water-based materials the speed of sound can be increased by the addition of alcohol-based substances (e.g., n-propanol[47,48], glycerol[49] etc), or decreased by the addition of oils[50]. Popular additives for tuning the acoustic attenuation include graphite[47,48] or $Al_2O_3$ powder[37,49], whilst for backscattering silica spheres or glass beads[48,51–53] are often used. These additives may also affect optical properties, further challenging the preparation of multimodal phantoms.

### Aqueous suspensions

Aqueous suspension phantoms are one of the most popular phantom types in optical imaging due to their ready availability, cost-effectiveness, easy preparation, and excellent reproducibility[18,32,61,62,43,54–60]. Water has negligible scattering and absorption properties in the visible wavelength range[63], but a lower speed of sound (1480 $m \cdot s^{-1}$) and acoustic attenuation coefficient (0.002 $dB \cdot cm^{-1} \cdot MHz^{-2}$ ) relative to most soft tissues[12,13]. The speed of sound can be increased by the addition of ethanol (e.g., 7.4% by mass for 1540 $m \cdot s^{-1}$)[64]. For tuning optical scattering properties, fat emulsions[28,29,58,30–33,54–57] or microspheres[59,60] are preferred, while optical absorption can be tuned by adding whole blood or extracted erythrocytes[56,59,65], inks[43,66,67], molecular dyes[61,62]. Blood-based phantoms[59,65,68–71] can also mimic changes in oxygen saturation ($SO_2$), by addition of oxygenating (e.g., oxygen) or deoxygenating compounds (e.g., yeast[65,68,71]). Due to their excellent reproducibility[30,31,42], aqueous phantoms with ink have been considered in several multi-laboratory studies[18,72].

Despite their advantages, liquid phantoms have a limited shelf life of only a few hours to days, with storage below 4°C and careful maintenance[73]. Moreover, mismatches of the refractive index and acoustic impedance of the container walls or embedded inclusions can cause optical and acoustic channelling artefacts, especially at the surfaces[74–76]. Water and water-based materials are also known to have a strong dependence on temperature, with the speed of sound in water varying up to 50 $m \cdot s^{-1}$ in the temperature range of 20–40°C[20].

### Hydrogels

Hydrogels refer to water-swollen, cross-linked polymer networks and can be formulated from natural or synthetic sources. The popularity of hydrogels for phantom fabrication stems from their well-characterized performance, ease of fabrication and flexibility in terms of architecture and tuning of intrinsic properties. They are largely optical transparent and optical and acoustic properties can be easily tuned (Table 1). 'Intelligent' hydrogels can also be sensitive to external stimuli, such as pH[77], temperature or light[78].

In the field of biophotonic phantoms, four main types of hydrogels have been used: (i) agarose[37,44,53,73,79–83]; (ii) gelatin[45,50,52,79,84–86]; (iii) polyacrylamide[87,88]; and (iv) poly(vinyl alcohol) (PVA)[89–93]. Agarose is a hydrophilic colloid that is derived from seaweed and red algae, whereas gelatin is a homogeneous colloid gel produced by physical, thermal, or chemical degradation of collagen extracted from animal tissues. Agarose and gelatin hydrogels are prepared by mixing with water, heating to crosslink, then cooling. Agarose gels exhibit a higher melting temperature (40˚C vs 90˚C) and higher stiffness, but lower toughness compared to gelatin[52]. Despite their widespread use in research settings, agar and gelatin gels suffer from

short-term stability[43,83], being highly susceptible to dehydration, bacterial ingrowth, thermal and mechanical damage, limiting reuse[94,95]. Extending longevity is possible by careful storage[51] and addition of chemicals such as formaldehyde[79] or benzalkonium chloride[49,96], though this increases fabrication complexity. Moreover, well defined inserts within hydrogels are usually short-lived due to diffusion of absorbers[97]. Targets can be encapsulated, but this creates refractive index mismatches and acoustic boundaries.

While agarose and gelatin are formed by physical crosslinking, polyacrylamide gels are formed by chemical reaction of acrylamide monomer and *N*, *N*'-methylene-bis-acrylamide and subsequent polymerization using a reaction initiator–activator pair. Polyacrylamide gels have higher melting temperature and optical transparency than gelatin or agarose[98]. However, their preparation process is more complex and requires a higher level of precautionary measures as polyacrylamide may contain residual amounts of the known neurotoxin acrylamide monomer[99]. Moreover, polyacrylamide gels are more likely to suffer from cluster formation resulting in structural inhomogeneities and have a more limited shelf life, ranging from a few hours upon air exposure to a few weeks in airtight containers[98]. A special, proprietary type of polyacrylamide called Zerdine™ forms the base material of a commercially available standard ultrasound phantom accredited by the American College of Radiology (ACR)[100].

PVA is a water soluble, biodegradable synthetic polymer derived from the hydrolysis of poly(vinyl acetate). The material is widely available, cost-effective, non-toxic and exhibits greater longevity and structural rigidity than agar-, gelatin- or polyacrylamide-based hydrogels[89,90]. While crosslinking can also occur chemically or by radiation, the base material is usually formed by physical crosslinking with alternate freezing (-20°C) and thawing (+20°C) cycles as it yields gels with higher mechanical strength and without toxic residues[101]. The optical[90], acoustic[93,102], mechanical[103], and electrical properties[104] can be tuned by changing: the number, length and rate of freeze and thaw cycles; the grade and concentration of the PVA; as well as additives and solvents[93,102,103,105–107]. By keeping the number of freeze-thaw cycles low and choosing a water/dimethyl sulfoxide (DMSO) mixture as a solvent, high optical transparency[108] and speed of sound[90] can be achieved. PVA phantoms can be stable for a 6-month period[109], if stored hydrated in sealed containers, yet the preparation process is time-consuming and tedious. Slight variations in fabrication can lead to inhomogeneities[91], compromising reproducibility. Moreover, as variation of preparation parameters affect acoustic, optical and mechanical parameters simultaneously, independent tunability is limited.

**Non-water-based materials**

Given the long-term stability and tunability concerns associated with aqueous suspensions and some hydrogels, the biophotonic community has also sought to adopt non-

water-based materials for phantom preparation. The most common examples are: (i) resins; (ii) room-temperature-vulcanizing (RTV) silicone; (iii) polyvinyl chloride plastisol (PVCP); and (iv) copolymer-in-oil materials.

First introduced by Firbank, Delpy[110,111] and Vernon[112] in the optical field, polyester[35,113–117], epoxy resin[35,117–121] and polyurethane[27,46,112,122,123] are transparent, solid materials that are formed by combining a resin with a hardener and are stable over years[46]. To create a homogenous, air-bubble-free base, the components are thoroughly mixed by mechanical stirring and/or sonication, then degassed and cured. Optical scattering is introduced by metal oxide powders[117] or microspheres[35,111,113,114,121] and absorption by pigment[124]- or dye-based inks[46,112,113,115,118,122] or (carbon) powders[120,125].

Polyester and epoxy-based materials are characterized by high speed of sound (>2000 $m \cdot s^{-1}$)[126], and have therefore been only considered as acoustic phantoms for hard tissues such as cortical or trabecular bone[126–129]. In contrast, polyurethane phantoms have a more tissue-like speed of sound (1400 - 1470 $m \cdot s^{-1}$) [130,131]. They also exhibit better compatibility with NIR dyes[46], less photobleaching and shorter hardening time[112] and have therefore been a popular choice in fluorescence imaging[27,122,123,132,133]. While final cured polyurethane is chemically inert, some of its unreacted ingredients such as isocyanates are toxic[134].

RTV silicone[40,135,144–149,136–143] exhibits similar properties to resin-based materials, but allows greater versatility in phantom design. It is composed of liquid polyorganosiloxanes that crosslink upon addition of a catalyst and is widely available in different hardness shores. Homogeneous fabrication is relatively simple: the materials and all additives are thoroughly mixed by mechanically stirring and/or sonication (often under addition of hexane to lower the viscosity of the mixture[142]), degassed and left to harden. Depending on silicone type and composition, the hardening process can take several days, but can be shortened to less than 24 h by heating.

The popularity of silicone as a phantom material arises from the tunability of optical properties, together with high stability (over 10 years depending on the formulation)[150]. Its low viscosity prior to curing affords flexible fabrication of anthropomorphic phantoms, e.g., for retina[151], bladder[143,152], artery[92], or skin[147,153,154], through molding[155,156] or spin-coating strategies[138,147]. Optical scattering may be tuned by addition of metal oxide powders[40,135–141,151,152] or size-controlled microspheres[40,135,142,154] and absorption by molecular dyes and inks such as india ink[140,147], carbon black[92] or alcohol soluble Nigrosin[138,140]. For mimicking tissue chromophores, coffee has been used to substitute melanin[139], freeze dried bovine haemoglobin[139] or zinc phthalocyanine[141] to mimic haemoglobin, yellow food dyes to imitate carotenoids[139], and infra-red dyes to mimic water[139]. Silicone shows high acoustic attenuation and low speed of sound (<1000 $m \cdot s^{-1}$)[99,130] with little tunability, so has limited potential for use in multimodal or hybrid applications. Optical and mechanical properties can be controlled

independently; the latter are comparable to tissues with high elastic moduli (e.g., ~100 kPa to ~5 MPa[156]). Care must be taken when tuning these properties as the polymer saturates at certain concentrations of external agents and can lose its integrity[139].

More recently, a suspension of a poly(vinyl chloride) (PVC) resin in a liquid plasticizer known as PVCP has been demonstrated for biophotonic phantoms. It is usually purchased as a two-part suspension of PVC resin and plasticizer forming a plastisol at room temperature[157]. While several preparation methods for PVCP phantoms have been proposed[97,158–161], the common procedure[162] involves sonication of additives with the plastisol mixture, degassing then gradual heating and subsequent cooling. The availability of various PVC-based formulations and additives gives scope for tuning the properties of the resulting material[163]. PVCP is generally optically transparent after preparation, so optical properties are adjusted by the addition of pigment-based absorbers[164] or black plastic colorant[159–161,165], and scatterers such as $TiO_2$[159,160,164,166] or ZiO[38,39]. The typical speed of sound is relatively low (1400 $m \cdot s^{-1}$)[158] but can be tuned by the addition of softener or hardener or by the type of plasticizer[161]. Solid PVCP inclusions within PVCP base material have been shown to be stable up to six months[159]. Unfortunately, PVCP suffers a major drawback, which is the lack of a supply chain with standard scientific suppliers[164]. Moreover, some plasticizers are based on phthalates, which can act as reproductive and developmental toxicants[167], subject to regulatory oversight in some regions.

Copolymer-in-oil materials are a relatively new class of phantom material based on thermoplastic styrenic elastomers, such as polystyrene-block-poly(ethylene-ran-butylene)-block-polystyrene (SEBS). Thermoplastic elastomers are composed of a rigid phase made of styrene structures and a rubber phase made of elastomeric structures and are easily processable as a melt at elevated temperatures[168]. Oil-based materials can be purchased off the shelf in the form of 'gel wax'[169–171] or can be manufactured from a choice of polymers and oil, where SEBS and mineral oil have proven popular[172–174]. The fabrication procedure typically requires sonication of additives with the plasticizer, mixing with the polymer and heating to the respective melting temperature, before degassing and curing. Oil-based materials are non-toxic, cost-effective, readily available, mechanically robust, have excellent temporal stability and short curing times[174,175]. Depending on their formulation, copolymer-in-oil materials can be optically transparent[169,176] with scattering and absorbing properties tuneable by additives such as oil-based dyes[169] and metal oxide powders[169,171]. The mechanical and acoustic properties are similar to breast fat[173] and can be modified by variation of polymer concentration[173,174], polymer[173] or plasticizer[174] type. The speed of sound also approaches soft tissue at 1500 $m \cdot s^{-1}$[177].

**3D printing for reproducing arbitrary shapes in physical phantoms**

In the past decade, additive manufacturing (AM), also known as 3D printing, has become a popular alternative to traditional casting and moulding for phantom fabrication[178]. AM refers to the process of adding materials in a layer-by-layer fashion providing a rapid, cost-efficient and high-fidelity method to create tissue-mimicking replicas of arbitrary shapes. 3D printing has been used to generate patient-specific phantoms from individual medical images, which is usually avoided in conventional fabrication due to the high tooling costs[179].

3D printing can be used in phantom fabrication through indirect (phantom mould) or direct[179–181] approaches. While 3D printing of moulds is widespread in optical imaging[143,170,182,183], direct printing of phantoms has been undertaken in a limited number of examples, mostly exploiting commercially available thermoplastic or photopolymer base materials[133,180,181,184–186]. Direct printing of common phantom materials, including hydrogels[187,188] and copolymer-in-oil[189] has also been explored (Supplementary Table 4). Tuning of optical properties is achieved by mixing scatterers[133,184,190] and absorbing agents[133,185,190] into the base materials prior to extrusion, or by combining different materials using dual extrusion 3D printing[185,189]. Multi-material AM has successfully been used to place heterogeneities within a phantom[191].

Despite the advantage of having a clear ground-truth design and robust manufacturing, limitations in printing methodology and available materials[192] must be overcome to enable 3D printing to realise its potential in phantom fabrication. Firstly, technical limitations of 3D printers may result in structural inhomogeneities, such as voids, air bubbles or surface roughness, which compromise the resulting phantom[193]. Non-invasive imaging (e.g., micro-computed tomography) can be used to verify the morphology of the printed object[181]. As the likelihood of these nonuniformities increases with the complexity of phantom, simple architectures are often chosen that do not account for *in vivo* complexity. Moreover, phantoms or phantom moulds can be damaged during the removal of the support material. Furthermore, only a restricted number of materials are available for AM phantom purposes. Using commercially available thermoplastic or photo-polymers with proprietary compositions is often accompanied with non-physiological mechanical and acoustic properties and limited tuning capabilities. With advances in printing technology, computer aided design (CAD) software and AM material research, these limitations may be overcome in future, thereby improving the current practice of phantom fabrication.

### Bioengineered tissues for reproducing biological complexity

With appropriate regulatory compliance, *ex vivo* tissues from bovine[194], porcine[195,196], chicken[197–200] and human sources[201,202] are often used as phantom substitutes, to better reflect biological heterogeneity. However, they can show high variability between samples as well as

discordance with *in vivo* optical properties if not perfused[203] or appropriately preserved[204], and also lack tunability. Bioengineered tissues, being composed of living matter, have emerged as alternative means to replicate biological complexity[182,205–208]. Engineered tissues are hybrid frameworks composed of cells seeded on porous scaffolds, which can be natural or synthetic[209]. Natural polymers offer greater similarity to *in vivo* tissue, and inherent bioactivity, whilst synthetic polymers provide better tunability of intrinsic characteristics[210]. Besides conventional seeding techniques, 3D-bioprinting has emerged as a precise strategy to create 3D functional living tissue constructs with customized architecture[210].

Bioengineered phantoms allow *in vitro* study of tissue physiology, function, and kinetics, and can act as a partial replacement for *in vivo* animal studies. Moreover, they provide a viable system for testing biological or environmental variables that are likely to influence the optical-imaging measurement[205]. Despite these promising prospects, adoption of these constructs to serve as biophotonic phantoms is still limited, due to time-consuming and costly preparation and maintenance as well as challenges with reproducibility, stability, accurate recapitulation of tissue physiology, and scalability. Nonetheless, as an active area of research, tissue bioengineering could lead to intriguing options for future application-specific phantoms.

**Phantoms improve the international standardisation of biophotonic instrumentations**

The establishment of international consensus standards represents a significant milestone in the maturation of a medical imaging modality. Typically, standards address key issues such as common terminology, safety evaluation procedures, and performance testing methods that can provide a foundation for future progress. Numerous safety and performance standards have been published for well-established medical imaging modalities such as ultrasound, MRI, and CT. These consensus standards provide a range of valuable information on concepts and methods for objective, quantitative assessment of fundamental performance in a rigorous and consistent manner. For example, key image quality characteristics are identified[211], or the morphology and physical properties of phantoms are addressed, as well as specific figures of merit and processing methods for quantifying them. Much of this information can be leveraged and adapted to advance translation in biophotonics.

For several clinically accepted optical technologies, such as endoscopy[212,213], pulse oximetry[214], and optical coherence tomography[215], device standards have already been developed. For several other modalities in biophotonics, there are established international efforts in standardisation. We provide three representative examples, to highlight the phantom requirements and the maturity of the respective standardisation initiatives.

**Diffuse optical imaging and spectroscopy**

Phantom-based performance characterisation and standardisation efforts have a long tradition in diffuse optics as related to: (i) imaging of optical absorption and scattering heterogeneities for normal tissue or pathology characterization, (ii) monitoring or imaging of functional changes in $O_2Hb$ and HHb concentrations in tissue, particularly brain or muscle (functional near-infrared spectroscopy, fNIRS, see Fig. 3a), and (iii) tissue oximetry. Phantoms for diffuse optics may thus require homogeneous or heterogeneous geometry, to mimic for example the layered structure of the head, as well as static or dynamic behaviours, to reflect functional changes in tissue properties (for details see Fig. 3b-e and Supplementary Table 3).

Besides the establishment of phantoms, there is the need to share standardised protocols that comprise guidelines (definitions of quantities and test metrics) and implementation (specification of phantoms and measurement procedures). Such protocols can be understood as precursors of potential future performance standards developed by standards bodies such as the International Electrotechnical Commission (IEC) or the International Organization for Standardization (ISO). In the past two decades, three protocols for performance evaluation in diffuse optics – BIP[216], MEDPHOT[19] and nEUROPt[72]– were elaborated in collaborative projects funded by the European Commission. BIP assesses Basic Instrumental Performance at the hardware level. An important test here is responsivity, the overall detection sensitivity, using a well characterized diffuse light source. MEDPHOT deals with the assessment of $\mu_a$ and $\mu_s$' in a homogeneous diffusive medium. It encompasses 5 tests, namely accuracy and linearity in the retrieval of these optical properties, temporal stability, uncertainty, and day-by-day reproducibility. nEUROPt analyses a heterogeneous problem with either localised or layered absorption changes. It prescribes 6 tests under 3 categories, namely sensitivity (contrast and contrast-to-noise ratio), localization (lateral resolution and depth selectivity), and quantitation (accuracy and linearity). These protocols were complemented with phantoms to implement the specific tests: solid homogeneous responsivity phantoms for BIP[216]; a matrix of 32 solid epoxy phantoms spanning a wide range of optical properties for MEDPHOT[19]; and a liquid intralipid/ink phantom with a suspended totally absorbing inclusion for nEUROPt[72], later supplemented by a solid epoxy-based version incorporating movable black inclusions[120] (Fig. 3b,d). Although these protocols were elaborated for specific applications (e.g., brain), they have been widely adopted in more than 50 studies across a range of applications.

The diffuse optics community has been active in pursuing multi-laboratory initiatives for phantom characterisation and joint testing of instruments. Nine institutions have characterised intralipid and ink for liquid phantoms, reaching an agreement within 2% for both $\mu_a$ and $\mu_s$'[18]. The BITMAP exercise is currently characterising 29 different instruments from 13 institutions

in 7 countries using the BIP, MEDPHOT and nEUROPt protocols, performing measurements on the same phantom kits, and providing open-data results for common analysis of the whole dataset with different models[217]. Furthermore, phantom-based comparison of devices was essential in multi-centre clinical trials such as SafeBoosC[218–220] and ACRIN[25].

Importantly, international efforts to create ISO/IEC documentary standards for fNIRS equipment[221] and cerebral tissue oximeters[222] as medical electrical devices have been undertaken by an ISO/IEC Joint Working Group (JWG) "Oximeters"[223,224], which includes scientific experts from the diffuse optics community. The main test in the fNIRS standard relies on a solid homogeneous turbid phantom with a changeable internal aperture to create a defined attenuation change. In the cerebral oximeter standard, an established liquid Intralipid / blood phantom[219] is proposed for accuracy verification, as an alternative to controlled human desaturation studies.

This example serves to illustrate the vital contribution of phantom-based testing of devices, which is now involved in shaping the regulatory process.

**Fluorescence guided surgery (FGS)**

FGS (Fig. 4a) is increasingly being utilized during surgical interventions, as it enables the surgeon to visualise features of the tissue in real-time with high contrast, while being low cost, safe and easy to use[225]. The earliest and most common use of FGS today is with indocyanine green (ICG), as a replacement for X-ray imaging of tissue vascular perfusion, and it is now being widely adopted for reconstructive surgery assessment of the capillary network function[226,227]. Being first approved by the FDA for retinal angiography in 1959, ICG now finds application in a wide variety of fields ranging from cardiology to neurosurgery[227]. Other exogenous contrast agents such as fluorescein and protoporphyrin IX fluorophore precursor aminolevulinic acid (ALA)[227] have led to wider adoption in neurosurgery[226,227]. Besides exogenous contrast agents, fluorescence signals can also occur as autofluorescence from endogenous tissue components (e.g., collagen, nicotinamide adenine dinucleotide (NADH), flavin adenine dinucleotide (FAD), or porphyrins), which can either be used as a diagnostic biomarker itself, or can be background clutter. [226,227].

Phantoms designed for FGS should ideally exhibit: (i) tissue-like absorption, scattering and fluorescent properties throughout the wavelength range of interest; (ii) application-specific fluorescence excitation and emission peaks that match the contrast agent used (in terms of spectrum and intensity); (iii) a reasonable fluorescence quantum yield and long-term photostability in diverse environmental conditions; (iv) capability for evaluating depth-dependent performance degradation; and (v) stable, tissue-like mechanical properties and anthropomorphic designs (e.g., for surgical training purposes).

To meet these requirements different materials have been tested, ranging from water[228], agar and gelatin[229–231], to polyester[54], silicone[231,232], dye-doped PMMA and metal-ion-glasses[233–235]and 3D-printable photopolymer[236]. Polyurethane[27,122,123,132,133] has been a popular choice due to its long term stability and negligible effect on the properties of embedded absorbers[46]. Since organic dyes such as ICG are not always sufficiently stable in phantom matrices, they are typically replaced by other fluorophores, such as the ICG-matching laser dye IR125[133] or quantum dots (QDots)[27,122,123,132,228]. Given the phantom requirements outlined, the majority of phantoms proposed for FGS have employed simple geometries[27,122,123,132,133,228,231,232,236], but a few studies created more complex, tissue-mimicking designs, such as breast[119,229,231].

Despite the promising potential of fluorescence imaging to improve visualisation of pathologies and clinical decision-making, standardisation is challenging as FGS performance depends not only on the data acquisition device and data processing methodology, but also on the fluorescent contrast agent and tissue being imaged[237,238]. The number of approved imaging systems has grown significantly, but the approval of devices is often tied to a specific

fluorophore[238], resulting in low flexibility for healthcare centres and compromising the translation of new contrast agents. Interestingly, the first regulatory approval that separated the fluorophore from the need for a specific imaging system occurred in the United States in 2017, for the use of Gleolan (ALA) in neurosurgery[239], which may increase the need for phantoms to validate and compare the performance of different systems that can be applied for use with the same fluorescent probe..

The need for FGS standardisation has long been identified[225,240–242]. and in 2017, a dedicated task group on FGS standardisation was formed within the American Association of Physicists in Medicine (AAPM). This task group published a "blue paper" outlining the key parameters, stakeholders, impacts and challenges of clinical FGS and its applications[238] and is currently compiling a consensus document on overall guidelines, test methods and suitable tissue simulating phantoms for advancing the field[243]. In parallel, Koch et al[237] proposed in 2019 standardisation parameters for fluorescence molecular imaging including suggestion of a composite phantom (Fig. 4b-d). The proposed phantom prototype originates from the work of Zhu et al.[123,244] (later adapted by Anastasopoulou et al[27]) who proposed a polyurethane-based phantom with $TiO_2$ as scatterer, and QDots as fluorophores and calibrated this phantom for emission radiance with International System of Units (SI) units of $mW \cdot sr^{-1} \cdot cm^{-2}$ by comparing its output to a reference source with known radiance. This phantom has been successfully employed in multi-device comparison studies[132,245,246] and developed further by various groups to e.g., to incorporate alcohol soluble nigrosin (mimicking lipid absorption spectrum) and hemin (mimicking haemoglobin absorption spectrum) as absorbers[27] or ICG as a fluorophore[133,245]. It was redesigned to enable parallel characterization of several performance metrics in a single or a few image acquisitions, including measurement of sensitivity, cross-talk, illumination homogeneity, dynamic range, dark current, resolution, and the effects of depth and optical properties[27,246]. A 3D printing approach[236] was also developed to create a more reproducible way of fabrication.[133]

This example illustrates the need for standards and test methods to ensure comparability of different clinical systems, which will increase confidence in the use of FGS for surgical decision making, ultimately broadening clinical adoption of the technology.

**Photoacoustic imaging**

PAI (Fig. 5a) is an emerging modality combining the high contrast of optical imaging with the spatial resolution of ultrasound. PAI has found clinical application thus far in both oncology and inflammatory diseases[247,248], primarily exploiting the absorption difference between $O_2Hb$ and HHb to derive functional biomarkers such as total haemoglobin concentration (ctHb) and $SO_2$.

PAI phantoms are particularly challenging to define. First, a PAI phantom should exhibit stable, tuneable, tissue-like behaviour in all relevant optical, acoustic and thermoelastic properties. Moreover, architectural flexibility of the base material is vital to satisfy the needs of the diverse landscape of instrument geometries. Many phantom materials have been tested for PAI, including hydrogels[95,249], PVA[90,91], silicone[250,251], PVCP[97,159,161,164–166] and copolymer-in-oil materials[172,177]. Inclusions have been made by embedding fluid-filled channels[161,252] or solid absorbers such as wires or filaments[253], or by creating simple[97,159,169] or more complex vessel-mimicking[165,170] inserts. PVCP[254] and copolymer-in-oil materials (Fig. 5b,c) appear to be most promising due to their high stability and excellent matching of both optical and acoustic properties in the tissue-mimicking range.

Standardisation in PAI is a relatively recent endeavour that has been driven by the community-led consensus-based effort IPASC: the International Photoacoustic Standardisation Consortium[255]. Founded in 2018, IPASC combines stakeholders from academia, industry and government laboratories aiming to reach consensus on standardised PAI performance test methods, test objects and data management for improving the quality of preclinical studies and reinforcing efforts in clinical translation[255]. These efforts have been streamlined into three thematic areas: (i) phantom development; (ii) data acquisition and management; and (iii) study design. The phantom development theme is currently evaluating the use of a copolymer-mineral oil phantom for multi-centre studies, where all constituent materials have defined chemical abstract service (CAS) numbers and are available from commercial chemistry suppliers, enabling local fabrication and testing. At present, a pilot study involving 13 partner labs is underway to assess the suitability of the material for widespread adoption in the research community. If successful, the outcomes will be used to establish performance test methods that can be extended into ongoing clinical trials of the modality.
This example highlights how phantoms can be used to facilitate technological progress in the early stages of clinical translation, thereby ensuring greater accuracy and precision of PAI data acquisition in future. **Future directions in phantom development**

The vast range of materials for biophotonic phantoms illustrates the challenge of finding consensus on standardized phantoms and test methods. Objective material evaluation is compromised due to variation in: (i) measurement and reporting of material characteristics; (ii) batch-to-batch variation of individual ingredients; (iii) methods of phantom preparation; (iv) environmental conditions during testing (e.g., temperature); and (v) test methods for phantom usage within a given modality. Moreover, fundamental differences in radiometric principles and practical implementations exist between different biophotonic approaches (e.g., contact-free and contact-based methods), which further hamper an encompassing validation approach. As illustrated in the presented examples, the imaging modality and application (tissue type or

indication for use) dictate the optimal phantom properties, with each example converging on a different solution.

Despite these hurdles, our examples demonstrate that achieving standardisation of phantoms and test methods in a given application is possible and can be valuable for regulatory approval of new clinical devices. While none of the presented material types satisfies all of the outlined requirements (Fig. 2), general recommendations can be made. For precision phantoms, solid, temporally stable non-water-based materials should be chosen. Here, epoxy-based materials have been adopted in diffuse optics and polyurethane has shown promise in FGS, while the substrate choice is perhaps not as critical as the mixing of the ingredients and verification of homogeneity and repeatability. It also seems likely that increasing use of 3D printing methods will eventually reduce variability, costs and production issues highlighted in this review. Copolymer-in-oil materials appear to be a promising option for PAI due to their tissue-mimicking broadly tunable optical, acoustic and mechanical properties, easy handling and non-toxic ingredients. These characteristics in combination with their potential 3D-printability suggest copolymer-in-oil materials may have the potential to become more widespread in biophotonic applications, particularly for those with a multi-modal aspect.

For biological accuracy phantoms, hydrogels are a suitable choice due to their excellent tissue-mimicking properties and biocompatibility, despite more complex handling requirements, allowing incorporation of tissue-derived components such as blood, fat or endogenous fluorescent molecules. Recent progress in the development of tough hydrogels[256] may provide strategies for creating water-based phantoms with higher temporal and mechanical stability. Tissue-engineered phantoms could also become a promising option as the technology advances, affording increased reproducibility and reduced costs. While the field is still in its infancy, new technologies such as 3D-bioprinting offer tremendous potential to create phantoms of enhanced biological realism with higher accuracy and precision. The importance of mimicking different target tissues as closely as possible becomes apparent in recent studies such as from Sjoding et al[257] highlighting the impact of different skin pigmentation on the accuracy of pulse oximeter readings.

While we highlighted ongoing efforts to achieve much-needed performance standards, there is also a growing need for new optical radiation safety standards for biophotonics. Existing standards that recommend maximum exposure limits for laser and non-coherent sources focus almost exclusively on damage of the eye and skin. Over the past twenty years, biophotonic systems have been developed for a wide range of internal applications, often through endoscopic or laparoscopic access[258,259]. Standards that address exposure limits in alternate tissue regions – including sensitive neural tissues and reproductive/gastrointestinal organs – may be needed to ensure patient safety, while avoiding overly restrictive limits that

adversely impact device performance. There is also rising interest in novel sources such as ultrashort pulsed lasers that are focused to achieve extremely high peak irradiance levels, enabling capabilities such as multi-photon imaging[260,261]. Other emerging approaches involve irradiation of new dye and nanoparticle contrast agents with continuous or pulsed lasers. Since the photothermal, photomechanical and photochemical damage mechanisms implicit in these technologies are not addressed by existing optical safety standards, additional standards should be developed.

Recently, the US FDA has introduced the Medical Device Development Tool (MDDT) programme[262], which is intended to encourage development of "regulatory science tools" that facilitate development and evaluation of clinical technologies. The program covers three types of tools – Clinical Outcome Assessments, Biomarker Tests, and Non-clinical Assessment Models (NAMs) – where the latter is defined as a technique that "measures or predicts device function or *in vivo* device performance" and includes phantoms and test targets. NAMs may reduce or eliminate the need for *in vivo* animal or human testing. Through the MDDT programme it is possible to qualify a phantom for a specific "context of use", so that it can be used in regulatory submissions without the need to reconfirm suitability and utility. The MDDT qualification process involves a proposal phase, an optional incubator phase, an optional pre-qualification package and a final qualification package. Some of the key considerations in evaluating submissions include tool validity and other performance characteristics, predictive ability, and extent of prediction. Overall, this new programme has the potential to reduce the burden of regulatory submissions while maintaining a high level of scientific rigour.

**The 4Cs for biophotonic standardisation**

As biophotonics moves along the translational pipeline toward clinical utility, the demand for standards grows. Within each modality, international standards should agree upon: (1) definitions of basic terminology used in the field; (2) performance metrics and test parameters suitable for the respective device; (3) a phantom material and geometric design suitable for the respective device; (4) standard operating procedures (SOPs) for the use of a given phantom with the device.

Ideally, phantom production should be scaled for manufacturing, for example by a commercial vendor, creating identical test objects with well controlled properties and geometries to comply with the recommendations. Similar commercially available phantoms exist for more mature technologies such as computed tomography, X-ray mammography, ultrasound and magnetic resonance imaging, which have been independently validated and conform to, for example, the Mammography Quality Standards Act (MQSA), and/or the ACR Quality Control

Programs[263]. In ultrasound, clear guidance on the development of tissue mimicking materials is given by the IEC standard 60601-2-37:2007,[264] which proposes a speed of sound of 1540 $ms^{-1}$ and an attenuation coefficient of 0.5–0.7 dB $cm^{-1}$ $MHz^{-1}$ in the frequency range of 2–15 MHz for conventional B-mode imaging. Adaptations exist for continuous-wave Doppler systems[265] and flow measurement systems[266]. A technical standard has been also published outlining methods for characterisation of ultrasound materials[267]. Agreement within the biophotonics community on required properties of tissue mimicking materials akin to that found in ultrasound would be advantageous from a translational perspective.

In many ways, these standards have been driven by the risks of the imaging system, with radiation risk being a key driver. As biophotonic systems are used to guide interpretation of biomarkers, biopsy, surgery or therapeutic interventions there are additional risks arising from inappropriate use of systems. As such, it is important to develop community standards that will eventually lead to broader safety guidance. Typically, commercial adoption drives the establishment of standards, but the two can be developed hand in hand, assisting the different communities participating, such as: (i) the company developing a quality management system; (ii) the regulatory bodies tasked with assessment; and (iii) the user base that benefits from confidence in the system performance.

Our presented examples highlighted the lengthy path towards achieving international standards. The complexity of the process increases when a modality is tied to an exogenous contrast agent, as shown in the example of FGS. Challenges include regulatory hurdles, lack of funding, lack of collaboration due to organizational issues and geographical barriers, and sometimes also lack of awareness of the importance of standardisation. To overcome the hurdles, characterisation is vital, and collaboration, communication, commitment from all participating bodies is required, which we refer to as the 4Cs for biophotonic standardisation.

**Characterisation.** Cutting across all phantom studies is the need for detailed characterisation and testing of reproducibility of phantom fabrication and test methods. Using ingredients available from standard scientific suppliers can help to minimise batch-to batch variations and maximise availability. Evaluating optical, acoustic and mechanical properties of phantom materials requires specialist equipment that is regularly calibrated. Metrology institutes are often capable of hosting such facilities and several already participate in biophotonic standardisation initiatives. Equipment hosted in research and industrial laboratories should ideally be cross-referenced to such reference institutes to determine the accuracy with which local characterisation can be undertaken for a given material. Ideally, traceability to the International System of Units (SI) should be achieved through an unbroken chain of comparisons (i.e., calibrations). Metrological traceability ensures that measurements are comparable across instruments, methodologies, times and locations. However, such rigorous

approach may not be always practicable or necessary, and there are only limited related examples for SI-traceability in biophotonics[122,244,268]. Another option of establishing long-term measurement repeatability is the use of materials that have been assigned with a conventionally true value to their physical properties of interest by the user community based on multi-laboratory assessments and that are produced under stable and controlled manufacturing conditions[269]. For example, intralipid-20% is considered as such a reference material by some research groups in the field of diffuse optics[31]. However, this approachis less favourable as it is highly sensitive to changes in the manufacturing process and does not compare to the accuracy achieved with certified reference materials as provided by e.g., national metrology institutes. In any case, careful implementation, documentation and understanding of the characterization measurement and its associated uncertainties is vital to ensure reproducibility and maximise the value of a phantom[270].

**Collaboration.** Increased multi-national collaboration – not only between research institutes, but also between the worlds of academia, industry, healthcare and government – is essential to find consensus on device handling and performance. A relatively small number of multi-centre studies have been performed in optical imaging[19,72,125,216,271]; increasing these efforts will harmonize data acquisition and analysis, making optical-imaging biomarkers more attractive for clinical decision making. Such collaborations require considerable organizational effort, meaning coordinated action is required. The presented examples highlight that this can be achieved by seeking guidance of an existing professional society (e.g., AAPM¸ SPIE), institution [e.g., Physikalisch-Technische Bundesanstalt (PTB, Germany), National Institute of Standards and Technology (NIST, US), National Physical Laboratory (NPL, UK)] or international standards organisations (e.g., ISO or IEC), or by founding a new independent community organisation (e.g., IPASC).

**Communication.** Clear communication and unrestricted flow of information between and within all participating bodies accelerates standardisation efforts. This is necessary for mediation and data sharing between different sites, but also - and most importantly - for raising the awareness of standardisation efforts. Here, international workshops[272,273] or conferences can be excellent fora, especially for exchanging standardisation experiences within and between different fields. Communication also means providing education and training for researchers and medical physicists, not only by respective manufacturers but also by specialized bodies[243]. Efforts from publishers are also needed in promoting recommendations within the relevant imaging communities and driving open access to publications and data.

**Commitment.** Active engagement from all entities is necessary to move the standardisation process forwards. Commitment means willingness to act, compromise and collaborate. In academic laboratories, emphasis is often placed on the design and development of a technology towards publication, rather than on its standardisation and clinical translation, despite the clear appetite for deploying biophotonics tools in the clinic. Efforts from funders to financially support projects focused on early stage multi-centre testing would enhance the reliability of optical-imaging technologies and support the widespread adoption of research achievements into clinical practice.

## Outlook

We believe that the principles embodied by the 4Cs strengthen efforts towards a future in which optical measures can be robust over time, between subjects, imaging sites, operators and manufacturers. These advances in phantom material development, manufacturing techniques, and design provide a valuable basis upon which to move forward the establishment of international biophotonic standards, facilitating the clinical adoption of optical imaging modalities.

**Disclosures of potential competing interests**

SEB has previously received research support from iThera Medical GmbH and PreXion Corporation, of which the photoacoustic imaging division was later acquired by CYBERDYNE Inc, which are both vendors of photoacoustic imaging instruments. BWP is financially involved as co-founder and president of DoseOptics LLC developing Cherenkov imaging in radiation therapy and QUEL Imaging LLC developing fluorescence imaging tools for surgery and photodynamic therapy. AP is co-founder of PIONIRS srl developing time-domain tissue oximeters.

**Disclaimer**

The mention of commercial products, their sources, or their use in connection with material reported herein is not to be construed as either an actual or implied endorsement of such products by the US Department of Health and Human Services. This article reflects the views of the authors and should not be construed to represent US FDA views or policies.

**Acknowledgements**

The authors thank Dr. William C. Vogt for his helpful advice on performance testing of medical imaging devices. LH is funded from NPL's MedAccel programme financed by the Department for Business, Energy and Industrial Strategy's Industrial Strategy Challenge Fund. SEB is funded by Cancer Research UK under grant numbers C47594/A16267 and C9545/A29580.

## Author contributions

S.E.B. and L.H. conceived the manuscript. L.H. researched and wrote the manuscript together with H.W., A.P., T.J.P., B.W.P. and S.E.B.. All authors discussed the content, reviewed and edited the manuscript and agreed with the final version of the manuscript.

## Additional information

Correspondence to Sarah E. Bohndiek.

**Bibliography**


1. Luker, G. D. & Luker, K. E. Optical imaging: Current applications and future directions. *Journal of Nuclear Medicine* vol. 49 1–4 (2008).

2. Tummers, W. S. *et al.* Regulatory Aspects of Optical Methods and Exogenous Targets for Cancer Detection. *Cancer Res* **77**, 2197–2206 (2017).

3. Nordstrom, R. J. Phantoms as standards in optical measurements. in (eds. Nordstrom, R. J. & Coté, G. L.) vol. 7906 79060H (International Society for Optics and Photonics, 2011).

4. Hwang, J., Ramella-Roman, J. C. & Nordstrom, R. Introduction: Feature Issue on Phantoms for the Performance Evaluation and Validation of Optical Medical Imaging Devices. *Biomed. Opt. Express* **3**, 1399 (2012).

5. Pogue, B. W. & Patterson, M. S. Review of tissue simulating phantoms for optical spectroscopy, imaging and dosimetry. *J. Biomed. Opt.* **11**, 041102 (2006).

6. Lamouche, G. *et al.* Review of tissue simulating phantoms with controllable optical, mechanical and structural properties for use in optical coherence tomography. *Biomed. Opt. Express* **3**, 1381 (2012).

7. Alexanderson-Rosas, E. *et al.* Current and future trends in multimodality imaging of coronary artery disease. *Expert Rev. Cardiovasc. Ther.* **13**, 715–731 (2015).

8. Yankeelov, T. E., Abramson, R. G. & Quarles, C. C. Quantitative multimodality imaging in cancer research and therapy. *Nature Reviews Clinical Oncology* vol. 11 670–680 (2014).

9. Kainz, W. *et al.* Advances in Computational Human Phantoms and Their Applications in Biomedical Engineering—A Topical Review. *IEEE Trans. Radiat. Plasma Med. Sci.* **3**, 1–23 (2018).

10. Jacques, S. L. Optical properties of biological tissues: a review. *Phys. Med. Biol.* **58**, R37–R61 (2013).

11. Cheong, W. F., Prahl, S. A. & Welch, A. J. A Review of the Optical Properties of Biological Tissues. *IEEE J. Quantum Electron.* **26**, 2166–2185 (1990).

12. Duck, F. A. & Institute of Physics and Engineering in Medicine (Great Britain). *Physical properties of tissue : a comprehensive reference book*.

13. Azhari, H. Appendix A: Typical Acoustic Properties of Tissues. in *Basics of Biomedical Ultrasound for Engineers* 313–314 (John Wiley & Sons, Inc., 2010).

doi:10.1002/9780470561478.app1.

14. Yao, D.-K., Zhang, C., Maslov, K. & Wang, L. V. Photoacoustic measurement of the Grüneisen parameter of tissue. *J. Biomed. Opt.* **19**, 017007 (2014).

15. Lemaillet, P., Bouchard, J.-P., Hwang, J. & Allen, D. W. Double-integrating-sphere system at the National Institute of Standards and Technology in support of measurement standards for the determination of optical properties of tissue-mimicking phantoms. *J. Biomed. Opt.* **20**, 121310 (2015).

16. Wilson, B. C. Measurement of Tissue Optical Properties: Methods and Theories. in *Optical-Thermal Response of Laser-Irradiated Tissue* 233–303 (Springer US, 1995). doi:10.1007/978-1-4757-6092-7_8.

17. Cubeddu, R., Pifferi, A., Taroni, P., Torricelli, A. & Valentini, G. Experimental test of theoretical models for time-resolved reflectance. *Med. Phys.* **23**, 1625–1633 (1996).

18. Spinelli, L. *et al.* Determination of reference values for optical properties of liquid phantoms based on Intralipid and India ink. *Biomed. Opt. Express* **5**, 2037 (2014).

19. Pifferi, A. *et al.* Performance assessment of photon migration instruments: The MEDPHOT protocol. *Appl. Opt.* **44**, 2104–2114 (2005).

20. Collins, D. E. ICRU REPORT 61: Tissue substitutes, phantoms and computational modelling in medical ultrasound. *Radiol. Technol.* **71**, 215–215 (1999).

21. Breitenberg, M. A. *NISTIR 7614 - The ABC's of Standards Activities*. (2009) doi:https://doi.org/10.6028/NIST.IR.7614.

22. J. Nordstrom, R. Translational Research and Standardization in Optical Imaging. *Curr. Mol. Imaging* **3**, 129–143 (2015).

23. *Investigational Device Exemptions (IDEs) for Early Feasibility Medical Device Clinical Studies, Including Certain First in Human (FIH) Studies | FDA*. https://www.fda.gov/regulatory-information/search-fda-guidance-documents/investigational-device-exemptions-ides-early-feasibility-medical-device-clinical-studies-including (2013).

24. *The 510(k) Program: Evaluating Substantial Equivalence in Premarket Notifications [510(k)] | FDA*. https://www.fda.gov/regulatory-information/search-fda-guidance-documents/510k-program-evaluating-substantial-equivalence-premarket-notifications-510k (2014).

25. Cerussi, A. E. *et al.* Tissue phantoms in multicenter clinical trials for diffuse optical

technologies. *Biomed. Opt. Express* **3**, 966 (2012).

26. Pikkula, B. M. *et al.* Instrumentation as a source of variability in the application of fluorescence spectroscopic devices for detecting cervical neoplasia. *J. Biomed. Opt.* **12**, 034014 (2007).

27. Anastasopoulou, M. *et al.* Comprehensive phantom for interventional fluorescence molecular imaging. *J. Biomed. Opt.* **21**, 091309 (2016).

28. Flock, S. T., Jacques, S. L., Wilson, B. C., Star, W. M. & van Gemert, M. J. C. Optical properties of intralipid: A phantom medium for light propagation studies. *Lasers Surg. Med.* **12**, 510–519 (1992).

29. van Staveren, H. J., Moes, C. J. M., van Marie, J., Prahl, S. A. & van Gemert, M. J. C. Light scattering in Intralipid-10% in the wavelength range of 400–1100 nm. *Appl. Opt.* **30**, 4507 (1991).

30. Di Ninni, P., Bérubé-Lauzière, Y., Mercatelli, L., Sani, E. & Martelli, F. Fat emulsions as diffusive reference standards for tissue simulating phantoms? *Appl. Opt.* **51**, 7176 (2012).

31. Di Ninni, P., Martelli, F. & Zaccanti, G. Intralipid: towards a diffusive reference standard for optical tissue phantoms. *Phys. Med. Biol.* **56**, N21–N28 (2011).

32. Michels, R., Foschum, F. & Kienle, A. Optical properties of fat emulsions. *Opt. Express* **16**, 5907 (2008).

33. Lepore, M. & Delfino, I. Intralipid-Based Phantoms for the Development of New Optical Diagnostic Techniques. *Open Biotechnol. J.* **13**, 163–172 (2019).

34. Vishwanath, K., Pogue, B. & Mycek, M.-A. Quantitative fluorescence lifetime spectroscopy in turbid media: comparison of theoretical, experimental and computational methods. *Phys. Med. Biol.* **47**, 3387–3405 (2002).

35. Firbank, M. *et al.* An improved design for a stable and reproducible phantom material for use in near-infrared spectroscopy and imaging. *Phys. Med. Biol.* **40**, 955–961 (1995).

36. Saager, R. B., Quach, A., Rowland, R. A., Baldado, M. L. & Durkin, A. J. Low-cost tissue simulating phantoms with adjustable wavelength-dependent scattering properties in the visible and infrared ranges. *J. Biomed. Opt.* **21**, 067001 (2016).

37. Ntombela, L., Adeleye, B. & Chetty, N. Low-cost fabrication of optical tissue phantoms for use in biomedical imaging. *Heliyon* **6**, (2020).

38. Wróbel, M. S. *et al.* Multi-layered tissue head phantoms for noninvasive optical diagnostics. in *Journal of Innovative Optical Health Sciences* vol. 8 8 (World Scientific Publishing Co. Pte Ltd, 2015).

39. Wróbel, M. S. *et al.* Use of optical skin phantoms for preclinical evaluation of laser efficiency for skin lesion therapy. *J. Biomed. Opt.* **20**, 085003 (2015).

40. de Bruin, D. M. *et al.* Optical phantoms of varying geometry based on thin building blocks with controlled optical properties. *J. Biomed. Opt.* **15**, 025001 (2010).

41. Huang, X. & El-Sayed, M. A. Gold nanoparticles: Optical properties and implementations in cancer diagnosis and photothermal therapy. *Journal of Advanced Research* vol. 1 13–28 (2010).

42. Di Ninni, P., Martelli, F. & Zaccanti, G. The use of India ink in tissue-simulating phantoms. *Opt. Express* **18**, 26854 (2010).

43. Madsen, S. J., Patterson, M. S. & Wilson, B. C. The use of India ink as an optical absorber in tissue-simulating phantoms. *Phys. Med. Biol.* **37**, 985–993 (1992).

44. Iizuka, M., Sherar, M. & Vitkin, I. Optical Phantom Materials for Near Infrared Laser Photocoagulation Studies. *Lasers Surg. Med.* **25**, (1999).

45. Vitkin, I. A., Wilson, B. C. & Anderson, R. R. Analysis of layered scattering materials by pulsed photothermal radiometry: application to photon propagation in tissue. *Appl. Opt.* **34**, 2973 (1995).

46. Moffitt, T., Chen, Y.-C. & Prahl, S. A. Preparation and characterization of polyurethane optical phantoms. *J. Biomed. Opt.* **11**, 041103 (2006).

47. Madsen, E. L., Zagzebski, J. A., Banjavie, R. A. & Jutila, R. E. Tissue mimicking materials for ultrasound phantoms. *Med. Phys.* **5**, 391–394 (1978).

48. Burlew, M. M., Madsen, E. L., Zagzebski, J. A., Banjavic, R. A. & Sum, S. W. A new ultrasound tissue-equivalent material. *Radiology* **134**, 517–520 (1980).

49. Ramnarine, K. V., Anderson, T. & Hoskins, P. R. Construction and geometric stability of physiological flow rate wall-less stenosis phantoms. *Ultrasound Med. Biol.* **27**, 245–250 (2001).

50. Madsen, E. L., Zagzebski, J. A. & Frank, G. R. Oil-in-gelatin dispersions for use as ultrasonically tissue-mimicking materials. *Ultrasound Med. Biol* **8**, 277–287 (1982).

51. Madsen, E. L., Frank, G. R. & Dong, F. Liquid or solid ultrasonically tissue-mimicking materials with very low scatter. *Ultrasound Med. Biol.* **24**, 535–542 (1998).

52. Madsen, E. L. *et al.* Tissue-mimicking oil-in-gelatin dispersions for use in heterogeneous elastography phantoms. *Ultrason. Imaging* **25**, 17–38 (2003).

53. D'Souza, W. D. *et al.* Tissue mimicking materials for a multi-imaging modality prostate phantom. *Med. Phys.* **28**, 688–700 (2001).

54. Quarto, G. *et al.* Recipes to make organic phantoms for diffusive optical spectroscopy. *Appl. Opt.* **52**, 2494–2502 (2013).

55. Merritt, S. *et al.* Comparison of Water and Lipid Content Measurements Using Diffuse Optical Spectroscopy and MRI in Emulsion Phantoms. *Technol. Cancer Res. Treat.* **2**, 563–569 (2003).

56. Linford, J., Shalev, S., Bews, J., Brown, R. & Schipper, H. Development of a tissue equivalent phantom for diaphanography. *Med. Phys.* **13**, 869–875 (1986).

57. Ebert, B. *et al.* Near-infrared fluorescent dyes for enhanced contrast in optical mammography: phantom experiments. *J. Biomed. Opt.* **6**, 134 (2001).

58. Cortese, L. *et al.* Liquid phantoms for near-infrared and diffuse correlation spectroscopies with tunable optical and dynamic properties. *Biomed. Opt. Express* **9**, 2068 (2018).

59. Hull, E. L., Nichols, M. G. & Foster, T. H. Quantitative broadband near-infrared spectroscopy of tissue-simulating phantoms containing erythrocytes. *Phys. Med. Biol.* **43**, 3381–3404 (1998).

60. Wang, D., Chen, Y. & Liu, J. T. C. A liquid optical phantom with tissue-like heterogeneities for confocal microscopy. *Biomed. Opt. Express* **3**, 3153 (2012).

61. Del Bianco, S. *et al.* Liquid phantom for investigating light propagation through layered diffusive media. *Opt. Express* **12**, 2102 (2004).

62. Moes, C. J. M., van Gemert, M. J. C., Star, W. M., Marijnissen, J. P. A. & Prahl, S. A. Measurements and calculations of the energy fluence rate in a scattering and absorbing phantom at 633 nm. *Appl. Opt.* **28**, 2292 (1989).

63. Hale, G. M. & Querry, M. R. Optical Constants of Water in the 200-nm to 200-μm Wavelength Region. *Appl. Opt.* **12**, 555 (1973).

64. Glacomini, A. Ultrasonic Velocity in Ethanol-Water Mixtures. *J. Acoust. Soc. Am.* **19**, 701–702 (1947).

65. Hunter, R. J., Patterson, M. S., Farrell, T. J. & Hayward, J. E. Haemoglobin oxygenation of a two-layer tissue-simulating phantom from time-resolved reflectance:

effect of top layer thickness. *Phys. Med. Biol.* **47**, 193–208 (2002).

66. Kimbrough, C. W., Hudson, S., Khanal, A., Egger, M. E. & McNally, L. R. Orthotopic pancreatic tumors detected by optoacoustic tomography using Syndecan-1. *J. Surg. Res.* **193**, 246–254 (2015).

67. Loginova, D. A., Sergeeva, E. A., Krainov, A. D., Agrba, P. D. & Kirillin, M. Y. Liquid optical phantoms mimicking spectral characteristics of laboratory mouse biotissues. *Quantum Electron.* **46**, 528–533 (2016).

68. Kleiser, S., Nasseri, N., Andresen, B., Greisen, G. & Wolf, M. Comparison of tissue oximeters on a liquid phantom with adjustable optical properties. *Biomed. Opt. Express* **7**, 2973 (2016).

69. Hyttel-Sorensen, S., Kleiser, S., Wolf, M. & Greisen, G. Calibration of a prototype NIRS oximeter against two commercial devices on a blood-lipid phantom. *Biomed. Opt. Express* **4**, 1662 (2013).

70. Kleiser, S., Hyttel-Sorensen, S., Greisen, G. & Wolf, M. Comparison of near-infrared oximeters in a liquid optical phantom with varying intralipid and blood content. in *Advances in Experimental Medicine and Biology* vol. 876 413–418 (Springer New York LLC, 2016).

71. Isler, H. *et al.* Liquid blood phantoms to validate NIRS oximeters: Yeast versus nitrogen for deoxygenation. in *Advances in Experimental Medicine and Biology* vol. 1072 381–385 (Springer New York LLC, 2018).

72. Wabnitz, H. *et al.* Performance assessment of time-domain optical brain imagers, part 2: nEUROPt protocol. *J. Biomed. Opt.* **19**, 086012 (2014).

73. Ohmae, E. *et al.* Stable tissue-simulating phantoms with various water and lipid contents for diffuse optical spectroscopy. *Biomed. Opt. Express* **9**, 5792 (2018).

74. Andersson-Engels, S., Berg, R. & Svanberg, S. Effects of optical constants on time-gated transillumination of tissue and tissue-like media. *J. Photochem. Photobiol. B Biol.* **16**, 155–167 (1992).

75. Pogue, B. W., Patterson, M. S., Jiang, H. & Paulsen, K. D. Initial assessment of a simple system for frequency domain diffuse optical tomography. *Phys. Med. Biol.* **40**, 1709–1729 (1995).

76. Cubeddu, R., Pifferi, A., Taroni, P., Torricelli, A. & Valentini, G. Time-resolved imaging on a realistic tissue phantom: μs′ and μa images versus time-integrated images. *Appl. Opt.* **35**, 4533 (1996).

77. Li, X. & Su, X. Multifunctional smart hydrogels: Potential in tissue engineering and cancer therapy. *Journal of Materials Chemistry B* vol. 6 4714–4730 (2018).

78. Khan, S., Ullah, A., Ullah, K. & Rehman, N. U. Insight into hydrogels. *Designed Monomers and Polymers* vol. 19 456–478 (2016).

79. Hall, T. J., Bilgen, M., Insana, M. F. & Krouskop, T. A. Phantom materials for elastography. *IEEE Trans. Ultrason. Ferroelectr. Freq. Control* **44**, 1355–1365 (1997).

80. Cubeddu, R., Pifferi, A., Taroni, P., Torricelli, A. & Valentini, G. A solid tissue phantom for photon migration studies. *Phys. Med. Biol.* **42**, 1971–1979 (1997).

81. Mustari, A. *et al.* Agarose-based tissue mimicking optical phantoms for diffuse reflectance spectroscopy. *J. Vis. Exp.* **2018**, e57578 (2018).

82. Wagnières, G. *et al.* An optical phantom with tissue-like properties in the visible for use in PDT and fluorescence spectroscopy. *Phys. Med. Biol.* **42**, 1415–1426 (1997).

83. Durkin, A. J., Jaikumar, S. & Richards-Kortum, R. Optically Dilute, Absorbing, and Turbid Phantoms for Fluorescence Spectroscopy of Homogeneous and Inhomogeneous Samples. *Appl. Spectrosc.* **47**, 2114–2121 (1993).

84. Saiko, G., Zheng, X., Betlen, A. & Douplik, A. Fabrication and optical characterization of gelatin-based phantoms for tissue oximetry. in *Advances in Experimental Medicine and Biology* vol. 1232 369–374 (Springer, 2020).

85. Hielscher, A. H., Liu, H., Chance, B., Tittel, F. K. & Jacques, S. L. Time-resolved photon emission from layered turbid media. *Appl. Opt.* **35**, 719 (1996).

86. Bush, N. L. & Hill, C. R. Gelatine-alginate complex gel: A new acoustically tissue-equivalent material. *Ultrasound Med. Biol.* **9**, 479–484 (1983).

87. McDonald, M., Lochhead, S., Chopra, R. & Bronskill, M. J. Multi-modality tissue-mimicking phantom for thermal therapy. *Phys. Med. Biol.* **49**, 2767–2778 (2004).

88. Geoghegan, R. *et al.* A tissue-mimicking prostate phantom for 980 nm laser interstitial thermal therapy. *Int. J. Hyperth.* **36**, 992–1001 (2019).

89. Fromageau, J., Brusseau, E., Vray, D., Gimenez, G. & Delachartre, P. Characterization of PVA cryogel for intravascular ultrasound elasticity imaging. *IEEE Trans. Ultrason. Ferroelectr. Freq. Control* **50**, 1318–24 (2003).

90. Kharine, A. *et al.* Poly(vinyl alcohol) gels for use as tissue phantoms in photoacoustic mammography. **48**, 357–370 (2003).

91. Xia, W. *et al.* Poly(vinyl alcohol) gels as photoacoustic breast phantoms revisited. *J.*

*Biomed. Opt.* **16**, 075002 (2011).

92. Bisaillon, C.-É., Dufour, M. L. & Lamouche, G. Artery phantoms for intravascular optical coherence tomography: healthy arteries. *Biomed. Opt. Express* **2**, 2599 (2011).

93. Devi, C. U., Vasu, R. M. & Sood, A. K. Design, fabrication, and characterization of a tissue-equivalent phantom for optical elastography. *J. Biomed. Opt.* **10**, 044020 (2005).

94. Culjat, M. O., Goldenberg, D., Tewari, P. & Singh, R. S. A Review of Tissue Substitutes for Ultrasound Imaging. *Ultrasound Med. Biol.* **36**, 861–873 (2010).

95. Cook, J. R., Bouchard, R. R. & Emelianov, S. Y. Tissue-mimicking phantoms for photoacoustic and ultrasonic imaging. *Biomed. Opt. Express* **2**, 3193 (2011).

96. Teirlinck, C. J. P. M. *et al.* Development of an example flow test object and comparison of five of these test objects, constructed in various laboratories. *Ultrasonics* **36**, 653–660 (1998).

97. Fonseca, M., Zeqiri, B., Beard, P. C. & Cox, B. T. Characterisation of a phantom for multiwavelength quantitative photoacoustic imaging. *Phys. Med. Biol.* **61**, 4950–4973 (2016).

98. Bini, M. G. *et al.* The Polyacrylamide as a Phantom Material for Electromagnetic Hyperthermia Studies. *IEEE Trans. Biomed. Eng.* **BME-31**, 317–322 (1984).

99. Zell, K., Sperl, J. I., Vogel, M. W., Niessner, R. & Haisch, C. Acoustical properties of selected tissue phantom materials for ultrasound imaging. *Phys. Med. Biol.* **52**, (2007).

100. General Purpose Ultrasound Phantom - CIRS. https://www.cirsinc.com/products/ultrasound/zerdine-hydrogel/general-purpose-ultrasound-phantom/.

101. Yang, X., Tong, Y. Y., Li, Z. C. & Liang, D. Aggregation-induced microgelation: A new approach to prepare gels in solution. *Soft Matter* **7**, 978–985 (2011).

102. Surry, K. J. M., Austin, H. J. B., Fenster, A. & Peters, T. M. Poly(vinyl alcohol) cryogel phantoms for use in ultrasound and MR imaging. *Phys. Med. Biol.* **49**, 5529–5546 (2004).

103. Wan, W. K., Campbell, G., Zhang, Z. F., Hui, A. J. & Boughner, D. R. Optimizing the tensile properties of polyvinyl alcohol hydrogel for the construction of a bioprosthetic heart valve stent. *J. Biomed. Mater. Res.* **63**, 854–861 (2002).

104. Goharian, M. *et al.* Modifying the MRI, elastic stiffness and electrical properties of

polyvinyl alcohol cryogel using irradiation. *Nucl. Instruments Methods Phys. Res. Sect. B Beam Interact. with Mater. Atoms* **263**, 239–244 (2007).

105. Hassan, C. M. & Peppas, N. A. Structure and applications of poly(vinyl alcohol) hydrogels produced by conventional crosslinking or by freezing/thawing methods. *Advances in Polymer Science* vol. 153 37–65 (2000).

106. Mori, Y., Tokura, H. & Yoshikawa, M. Properties of hydrogels synthesized by freezing and thawing aqueous polyvinyl alcohol solutions and their applications. *J. Mater. Sci.* **32**, 491–496 (1997).

107. Nagura, M., Nagura, M. & Ishikawa, H. State of water in highly elastic poly(vinyl alcohol) hydrogels prepared by repeated freezing and melting. *Polym. Commun. Guildf.* **25**, 313–314 (1984).

108. Hyon, S. H., Cha, W. I. & Ikada, Y. Preparation of transparent poly(vinyl alcohol) hydrogel. *Polym. Bull.* **22**, 119–122 (1989).

109. Mano, I., Goshima, H., Nambu, M. & Iio, M. New polyvinyl alcohol gel material for MRI phantoms. *Magn. Reson. Med.* **3**, 921–926 (1986).

110. Firbank, M. J. An improved design for a stable a reproducible phantom material for use in near infra red spectroscopy and imaging. *Artic. Phys. Med. Biol.* (1995) doi:10.1088/0031-9155/40/5/016.

111. Firbank, M., Oda, M. & Delpy, D. T. An improved design for a stable and reproducible phantom material for use in near-infrared spectroscopy and imaging. *Phys. Med. Biol.* **40**, 955–961 (1995).

112. Vernon, M. L., Fréchette, J., Painchaud, Y., Caron, S. & Beaudry, P. Fabrication and characterization of a solid polyurethane phantom for optical imaging through scattering media. *Appl. Opt.* **38**, 4247 (1999).

113. Sukowski, U., Schubert, F., Grosenick, D. & Rinneberg, H. Preparation of solid phantoms with defined scattering and absorption properties for optical tomography. *Phys. Med. Biol.* **41**, 1823–1844 (1996).

114. Firbank, M. & Delpy, D. T. A phantom for the testing and calibration of near infra-red spectrometers. *Phys. Med. Biol.* **39**, 1509–1513 (1994).

115. Hebden, J. C., Hall, D. J., Firbank, M. & Delpy, D. T. Time-resolved optical imaging of a solid tissue-equivalent phantom. *Appl. Opt.* **34**, 8038 (1995).

116. Hebden, J. C. *et al.* An electrically-activated dynamic tissue-equivalent phantom for

assessment of diffuse optical imaging systems. *Phys. Med. Biol.* **53**, 329–337 (2008).

117. Krauter, P. *et al.* Optical phantoms with adjustable subdiffusive scattering parameters. *J. Biomed. Opt.* **20**, 105008 (2015).

118. Koh, P. H., Elwell, C. E. & Delpy, D. T. Development of a dynamic test phantom for optical topography. in *Advances in Experimental Medicine and Biology* vol. 645 141–146 (Springer, Boston, MA, 2009).

119. Netz, U. J., Toelsner, J. & Bindig, U. Calibration standards and phantoms for fluorescence optical measurements. *Med. Laser Appl.* **26**, 101–108 (2011).

120. Pifferi, A. *et al.* Mechanically switchable solid inhomogeneous phantom for performance tests in diffuse imaging and spectroscopy. *J. Biomed. Opt.* **20**, 121304 (2015).

121. Avanaki, M. R. N., Podoleanu, A. G., Price, M. C., Corr, S. A. & Hojjatoleslami, S. A. Two applications of solid phantoms in performance assessment of optical coherence tomography systems. *Appl. Opt.* **52**, 7054–7061 (2013).

122. Zhu, B., Tan, I. C., Rasmussen, J. C. & Sevick-Mraca, E. M. Validating the sensitivity and performance of near-infrared fluorescence imaging and tomography devices using a novel solid phantom and measurement approach. *Technol. Cancer Res. Treat.* **11**, 95–104 (2012).

123. Zhu, B., Rasmussen, J. C. & Sevick-Muraca, E. M. A matter of collection and detection for intraoperative and noninvasive near-infrared fluorescence molecular imaging: To see or not to see? *Med. Phys.* **41**, (2014).

124. Bae, Y., Son, T., Park, J. & Jung, B. Fabrication of a thin-layer solid optical tissue phantom by a spin-coating method: pilot study. *J. Biomed. Opt.* **18**, 025006 (2013).

125. Swartling, J., Dam, J. S. & Andersson-Engels, S. Comparison of spatially and temporally resolved diffuse-reflectance measurement systems for determination of biomedical optical properties. *Appl. Opt.* **42**, 4612 (2003).

126. Clarke, A. J., Evans, J. A., Truscott, J. G., Milner, R. & Smith, M. A. *A phantom for quantitative ultrasound of trabecular bone*. *Phys. Med. Biol* vol. 39 (1994).

127. Tatarinov, A., Pontaga, I. & Vilks, U. *Modeling the influence of mineral content and porosity on ultrasound parameters in bone by using synthetic phantoms*. *Mechanics of Composite Materials* vol. 35 (1999).

128. Falardeau, T. & Belanger, P. Ultrasound tomography in bone mimicking phantoms:

Simulations and experiments. *J. Acoust. Soc. Am.* **144**, 2937–2946 (2018).

129. Wydra, A. & Maev, R. G. A novel composite material specifically developed for ultrasound bone phantoms: cortical, trabecular and skull. *Phys. Med. Biol.* **58**, N303–N319 (2013).

130. Cafarelli, A., Miloro, P., Verbeni, A., Carbone, M. & Menciassi, A. Speed of sound in rubber-based materials for ultrasonic phantoms. *J. Ultrasound* **19**, 251–256 (2016).

131. Goldstein, A. The effect of acoustic velocity on phantom measurements. *Ultrasound Med. Biol.* **26**, 1133–1143 (2000).

132. Gorpas, D., Koch, M., Anastasopoulou, M., Klemm, U. & Ntziachristos, V. Benchmarking of fluorescence cameras through the use of a composite phantom. *J. Biomed. Opt.* **22**, 016009 (2017).

133. Ruiz, A. J. *et al.* Indocyanine green matching phantom for fluorescence-guided surgery imaging system characterization and performance assessment. *J. Biomed. Opt.* **25**, 1 (2020).

134. C Dernehl. Health Hazards Associated With Polyurethane Foams - PubMed. *J Occup Med.* 59–62 (1966).

135. Bays, R. *et al.* Three-dimensional optical phantom and its application in photodynamic therapy. *Lasers Surg. Med.* **21**, 227–234 (1997).

136. Beck, G. C., Akgün, N., Rück, A. & Steiner, R. Design and characterisation of a tissue phantom system for optical diagnostics. *Lasers Med. Sci.* **13**, 160–171 (1998).

137. Lualdi, M., Colombo, A., Farina, B., Tomatis, S. & Marchesini, R. A phantom with tissue-like optical properties in the visible and near infrared for use in photomedicine. *Lasers Surg. Med.* **28**, 237–243 (2001).

138. Greening, G. J. *et al.* Characterization of thin poly(dimethylsiloxane)-based tissue-simulating phantoms with tunable reduced scattering and absorption coefficients at visible and near-infrared wavelengths. *J. Biomed. Opt.* **19**, 115002 (2014).

139. Saager, R. B., Quach, A., Kennedy, G. T., Tromberg, B. J. & Durkin, A. J. From theory to practice: the broadening role of polydimethylsiloxane phantoms as an intermediary between model validation and instrument performance testing (Conference Presentation). in *Design and Quality for Biomedical Technologies IX* (eds. Raghavachari, R., Liang, R. & Pfefer, T. J.) vol. 9700 15 (SPIE, 2016).

140. Saager, R. B. *et al.* Multilayer silicone phantoms for the evaluation of quantitative

optical techniques in skin imaging. in *Design and Performance Validation of Phantoms Used in Conjunction with Optical Measurement of Tissue II* (ed. Nordstrom, R. J.) vol. 7567 756706 (SPIE, 2010).

141. Monte, A. F. G., Reis, A. F., Cruz Junior, L. B. & Antunes, A. Preparation and quantitative characterization of polydimethylsiloxane optical phantoms with zinc-phthalocyanine dye absorbers. *Appl. Opt.* **57**, 5865 (2018).

142. Bisaillon, C. E., Lamouche, G., Maciejko, R., Dufour, M. & Monchalin, J. P. Deformable and durable phantoms with controlled density of scatterers. *Phys. Med. Biol.* **53**, (2008).

143. Smith, G. T., Lurie, K. L., Zlatev, D. V., Liao, J. C. & Ellerbee Bowden, A. K. Multimodal 3D cancer-mimicking optical phantom. *Biomed. Opt. Express* **7**, 648 (2016).

144. Bellan, L. M. *et al.* Fabrication of an artificial 3-dimensional vascular network using sacrificial sugar structures. *Soft Matter* **5**, 1354–1357 (2009).

145. Curatolo, A., Kennedy, B. F. & Sampson, D. D. Structured three-dimensional optical phantom for optical coherence tomography. *Opt. Express* **19**, 19480 (2011).

146. Agrawal, A., Pfefer, T. J., Gilani, N. & Drezek, R. Three-dimensional characterization of optical coherence tomography point spread functions with a nanoparticle-embedded phantom. *Opt. Lett.* **35**, 2269 (2010).

147. Park, J., Ha, M., Yu, S. & Jung, B. Fabrication of various optical tissue phantoms by the spin-coating method. *J. Biomed. Opt.* **21**, 065008 (2016).

148. Sekar, S. K. V. *et al.* Solid phantom recipe for diffuse optics in biophotonics applications: a step towards anatomically correct 3D tissue phantoms. *Biomed. Opt. Express* **10**, 2090 (2019).

149. Little, C. D. *et al.* Micron resolution, high-fidelity three-dimensional vascular optical imaging phantoms. *J. Biomed. Opt.* **24**, 1 (2019).

150. Homma, H., Mirley, C. L., Ronzello, J. A. & Boggs, S. A. Field and laboratory aging of RTV silicone insulator coatings. *IEEE Trans. Power Deliv.* **15**, 1298–1303 (2000).

151. Baxi, J. *et al.* Retina-simulating phantom for optical coherence tomography. *J. Biomed. Opt.* **19**, 021106 (2013).

152. Lurie, K. L., Smith, G. T., Khan, S. A., Liao, J. C. & Ellerbee, A. K. Three-dimensional, distendable bladder phantom for optical coherence tomography and white light

cystoscopy. *J. Biomed. Opt.* **19**, 036009 (2014).

153. Lualdi, M., Colombo, A., Mari, A., Tomatis, S. & Marchesini, R. Development of simulated pigmented lesions in an optical skin-tissue phantom: Experimental measurements in the visible and near infrared. *J. Laser Appl.* **14**, 122–127 (2002).

154. Diao, D. Y. *et al.* Durable rough skin phantoms for optical modeling. *Phys. Med. Biol.* **59**, 485–492 (2014).

155. Oldenburg, A. L., Toublan, F. J.-J., Suslick, K. S., Wei, A. & Boppart, S. A. Magnetomotive contrast for in vivo optical coherence tomography. *Opt. Express* **13**, 6597 (2005).

156. Kennedy*, B. F., Hillman, T. R., McLaughlin, R. A., Quirk, B. C. & Sampson, D. D. In vivo dynamic optical coherence elastography using a ring actuator. *Opt. Express* **17**, 21762 (2009).

157. Davis, D., McConnell, R., MF Meyer Jr - US Patent 4, 401,720 & 1983, undefined. *Poly (vinyl chloride) plastisol compositions*. *Google Patents* https://patents.google.com/patent/US4401720A/en (1982).

158. Maggi, L. *et al.* Ultrasonic Attenuation and Speed in Phantoms Made of PVCP and Evaluation of Acoustic and Thermal Proper-ties of Ultrasonic Phantoms Made of polyvinyl chloride-plastisol (PVCP).

159. Bohndiek, S. E., Bodapati, S., Van De Sompel, D., Kothapalli, S.-R. R. & Gambhir, S. S. Development and Application of Stable Phantoms for the Evaluation of Photoacoustic Imaging Instruments. *PLoS One* **8**, 1–14 (2013).

160. Spirou, G., Oraevsky, A., Vitkin, I. & Whelan, W. Optical and acoustic properties at 1064 nm of polyvinyl chloride-plastisol for use as a tissue phantom in biomedical optoacoustics. *Phys Med Biol* **50**, (2005).

161. Vogt, W. C., Jia, C., Wear, K. A., Garra, B. S. & Joshua Pfefer, T. Biologically relevant photoacoustic imaging phantoms with tunable optical and acoustic properties. *J. Biomed. Opt.* **21**, 101405 (2016).

162. Bakaric, M., Miloro, P., Zeqiri, B., Cox, B. T. & Treeby, B. E. The Effect of Curing Temperature and Time on the Acoustic and Optical Properties of PVCP. *IEEE Trans. Ultrason. Ferroelectr. Freq. Control* **67**, 505–512 (2020).

163. Rybachuk, G. V., Kozlova, I. I., Mozzhukhin, V. B. & Guzeev, V. V. PVC plastisols: Preparation, properties, and application. *Polym. Sci. - Ser. C* **49**, 6–12 (2007).

164. Fonseca, M., Zeqiri, B., Beard, P. & Cox, B. Characterisation of a PVCP-based tissue-mimicking phantom for quantitative photoacoustic imaging. **9539**, 953911 (2015).

165. Dantuma, M., van Dommelen, R. & Manohar, S. Semi-anthropomorphic photoacoustic breast phantom. *Biomed. Opt. Express* **10**, 5921–5939 (2019).

166. Jeong, E. *et al.* Fabrication and characterization of PVCP human breast tissue-mimicking phantom for photoacoustic imaging. *BioChip J.* **11**, 67–75 (2017).

167. Heudorf, U., Mersch-Sundermann, V. & Angerer, J. Phthalates: Toxicology and exposure. *Int. J. Hyg. Environ. Health* **210**, 623–634 (2007).

168. Legge, N. R.; Holden, G.; Schroeder, H. E. Thermoplastic Elastomers. *Hanser:Munich* (1996).

169. Maneas, E. *et al.* Gel wax-based tissue-mimicking phantoms for multispectral photoacoustic imaging. *Biomed. Opt. Express* **9**, 1151 (2018).

170. Maneas, E. *et al.* Anatomically realistic ultrasound phantoms using gel wax with 3D printed moulds. *Phys. Med. Biol.* **63**, 015033 (2018).

171. Jones, C. J. M. & Munro, P. R. T. Stability of gel wax based optical scattering phantoms. *Biomed. Opt. Express* **9**, 3495–3502 (2018).

172. Grillo, F. W., Cabrelli, L. C., Sampaio, D. R. T., Carneiro, A. A. O. & Pavan, T. Z. Glycerol in oil-based phantom with improved performance for photoacoustic imaging. *IEEE Int. Ultrason. Symp. IUS* 1–4 (2017) doi:10.1109/ULTSYM.2017.8091705.

173. Cabrelli, L. C. *et al.* Stable phantom materials for ultrasound and optical imaging. *Phys. Med. Biol.* **62**, 432–447 (2017).

174. Oudry, J., Bastard, C., Miette, V., Willinger, R. & Sandrin, L. Copolymer-in-oil phantom materials for elastography. *Ultrasound Med. Biol.* **35**, 1185–97 (2009).

175. Suzuki, A. *et al.* Oil Gel-Based Phantom for Evaluating Quantitative Accuracy of Speed of Sound Measured in Ultrasound Computed Tomography. *Ultrasound Med. Biol.* **45**, 2554–2567 (2019).

176. Oudry, J. *et al.* Cross-validation of magnetic resonance elastography and ultrasound-based transient elastography: A preliminary phantom study. *J. Magn. Reson. Imaging* **30**, 1145–1150 (2009).

177. Cabrelli, L. C., Grillo, F. W., Sampaio, D. R. T., Carneiro, A. A. O. & Pavan, T. Z. Acoustic and Elastic Properties of Glycerol in Oil-Based Gel Phantoms. *Ultrasound Med. Biol.* **43**, 2086–2094 (2017).

178. Wang, K., Ho, C. C., Zhang, C. & Wang, B. A Review on the 3D Printing of Functional Structures for Medical Phantoms and Regenerated Tissue and Organ Applications. *Engineering* **3**, 653–662 (2017).

179. Filippou, V. & Tsoumpas, C. Recent advances on the development of phantoms using 3D printing for imaging with CT, MRI, PET, SPECT, and ultrasound. *Med. Phys.* **45**, e740–e760 (2018).

180. Afshari, A. *et al.* Cerebral oximetry performance testing with a 3D-printed vascular array phantom. *Biomed. Opt. Express* **10**, 3731 (2019).

181. Wang, J. *et al.* Three-dimensional printing of tissue phantoms for biophotonic imaging. *Opt. Lett.* **39**, 3010 (2014).

182. Kim, H., Hau, N. T., Chae, Y.-G., Lee, B. & Kang, H. W. 3D printing-assisted fabrication of double-layered optical tissue phantoms for laser tattoo treatments. *Lasers Surg. Med.* **48**, 392–399 (2016).

183. Arconada-Alvarez, S. J., Lemaster, J. E., Wang, J. & Jokerst, J. V. The development and characterization of a novel yet simple 3D printed tool to facilitate phantom imaging of photoacoustic contrast agents. *Photoacoustics* **5**, 17–24 (2017).

184. Ghassemi, P. *et al.* Rapid prototyping of biomimetic vascular phantoms for hyperspectral reflectance imaging. *J. Biomed. Opt.* **20**, 121312 (2015).

185. Diep, P. *et al.* Three-dimensional printed optical phantoms with customized absorption and scattering properties. *Biomed. Opt. Express* **6**, 4212 (2015).

186. Pinkert, M. A., Cox, B. L., Dai, B., Hall, T. J. & Eliceiri, K. W. 3-D-Printed Registration Phantom for Combined Ultrasound and Optical Imaging of Biological Tissues. *Ultrasound Med. Biol.* **46**, 1808–1814 (2020).

187. Aljohani, W. *et al.* Three-dimensional printing of alginate-gelatin-agar scaffolds using free-form motor assisted microsyringe extrusion system. *J. Polym. Res.* **25**, (2018).

188. Li, J., Wu, C., Chu, P. K. & Gelinsky, M. 3D printing of hydrogels: Rational design strategies and emerging biomedical applications. *Materials Science and Engineering R: Reports* vol. 140 100543 (2020).

189. Dong, E. *et al.* Three-dimensional fuse deposition modeling of tissue-simulating phantom for biomedical optical imaging. *J. Biomed. Opt.* **20**, 121311 (2015).

190. Corcoran, A., Muyo, G., Van Hemert, J., Gorman, A. & Harvey, A. R. Application of a wide-field phantom eye for optical coherence tomography and reflectance imaging. *J.*

*Mod. Opt.* **62**, 1828–1838 (2015).

191. Bentz, B. Z. *et al.* Printed optics: phantoms for quantitative deep tissue fluorescence imaging. *Opt. Lett.* **41**, 5230 (2016).

192. Oropallo, W. & Piegl, L. A. Ten challenges in 3D printing. *Eng. Comput.* **32**, 135–148 (2016).

193. Gordeev, E. G., Galushko, A. S. & Ananikov, V. P. Improvement of quality of 3D printed objects by elimination of microscopic structural defects in fused deposition modeling. *PLoS One* **13**, e0198370 (2018).

194. Kienle, A., Patterson, M. S., Ott, L. & Steiner, R. Determination of the scattering coefficient and the anisotropy factor from laser Doppler spectra of liquids including blood. *Appl. Opt.* **35**, 3404 (1996).

195. Grabtchak, S., Montgomery, L. G. & Whelan, W. M. Optical absorption and scattering properties of bulk porcine muscle phantoms from interstitial radiance measurements in 650–900 nm range. *Phys. Med. Biol.* **59**, 2431–2444 (2014).

196. Grabtchak, S., Tonkopi, E. & Whelan, W. M. Optical detection of gold nanoparticles in a prostate-shaped porcine phantom. *J. Biomed. Opt.* **18**, 077005 (2013).

197. Shen, Y., Liu, Y., Ma, C. & Wang, L. V. Focusing light through biological tissue and tissue-mimicking phantoms up to 9.6 cm in thickness with digital optical phase conjugation. *J. Biomed. Opt.* **21**, 085001 (2016).

198. McDowell, E. J. *et al.* Turbidity suppression from the ballistic to the diffusive regime in biological tissues using optical phase conjugation. *J. Biomed. Opt.* **15**, 025004 (2010).

199. Stockbridge, C. *et al.* Focusing through dynamic scattering media. *Opt. Express* **20**, 15086 (2012).

200. Demos, S., Radousky, H. & Alfano, R. Deep subsurface imaging in tissues using spectral and polarization filtering. *Opt. Express* **7**, 23 (2000).

201. Yoon, J. *et al.* A clinically translatable hyperspectral endoscopy (HySE) system for imaging the gastrointestinal tract. *Nat. Commun.* **10**, 1–13 (2019).

202. Parot, V. *et al.* Photometric stereo endoscopy. *J. Biomed. Opt.* **18**, 1 (2013).

203. Leopaldi, A. M. *et al.* In vitro hemodynamics and valve imaging in passive beating hearts. *J. Biomech.* **45**, 1133–1139 (2012).

204. Eshmuminov, D. *et al.* An integrated perfusion machine preserves injured human livers for 1 week. *Nat. Biotechnol.* **38**, 189–198 (2020).

205. Sokolov, K. *et al.* Realistic three-dimensional epithelial tissue phantoms for biomedical optics. *J. Biomed. Opt.* **7**, 148 (2002).

206. Nieman, L., Myakov, A., Aaron, J. & Sokolov, K. Optical sectioning using a fiber probe with an angled illumination-collection geometry: Evaluation in engineered tissue phantoms. *Appl. Opt.* **43**, 1308–1319 (2004).

207. Robichaux Viehoever, A., Anderson, D., Jansen, D. & Mahadevan-Jansen, A. Organotypic Raft Cultures as an Effective In Vitro Tool for Understanding Raman Spectral Analysis of Tissue¶. *Photochem. Photobiol.* **78**, 517–524 (2007).

208. Liu, Y., Kim, Y. L. & Backman, V. Development of a bioengineered tissue model and its application in the investigation of the depth selectivity of polarization gating. *Appl. Opt.* **44**, 2288–2299 (2005).

209. Li, Z. & Kawashita, M. Current progress in inorganic artificial biomaterials. *Journal of Artificial Organs* vol. 14 163–170 (2011).

210. Murphy, S. V. & Atala, A. 3D bioprinting of tissues and organs. *Nature Biotechnology* vol. 32 773–785 (2014).

211. Pfefer, J. & Agrawal, A. A review of consensus test methods for established medical imaging modalities and their implications for optical coherence tomography. in *Design and Quality for Biomedical Technologies V* (eds. Raghavachari, R. & Liang, R.) vol. 8215 82150D (SPIE, 2012).

212. *ISO - ISO 8600-5:2020 - Optics and photonics — Medical endoscopes and endotherapy devices — Part 5: Determination of optical resolution of rigid endoscopes with optics*. https://www.iso.org/standard/65019.html (2020).

213. *ISO - ISO 8600-3:2019 - Endoscopes — Medical endoscopes and endotherapy devices — Part 3: Determination of field of view and direction of view of endoscopes with optics*. https://www.iso.org/standard/65018.html (2019).

214. *ISO - ISO 80601-2-61:2017 - Medical electrical equipment — Part 2-61: Particular requirements for basic safety and essential performance of pulse oximeter equipment*. https://www.iso.org/standard/67963.html (2017).

215. *ISO - ISO 16971:2015 - Ophthalmic instruments — Optical coherence tomograph for the posterior segment of the human eye*. https://www.iso.org/standard/58076.html (2015).

216. Wabnitz, H. *et al.* Performance assessment of time-domain optical brain imagers, part 1: basic instrumental performance protocol. *J. Biomed. Opt.* **19**, 086010 (2014).

217. Lanka, P. *et al.* The BITMAP exercise: a multi-laboratory performance assessment campaign of diffuse optical instrumentation. in *Diffuse Optical Spectroscopy and Imaging VII* (eds. Dehghani, H. & Wabnitz, H.) vol. Part F142-ECBO 2019 44 (SPIE, 2019).

218. Hansen, M. L. *et al.* Cerebral near-infrared spectroscopy monitoring versus treatment as usual for extremely preterm infants: A protocol for the SafeBoosC randomised clinical phase III trial. *Trials* **20**, (2019).

219. Kleiser, S., Nasseri, N., Andresen, B., Greisen, G. & Wolf, M. Comparison of tissue oximeters on a liquid phantom with adjustable optical properties. *Biomed. Opt. Express* **7**, 2973 (2016).

220. Kleiser, S. *et al.* Comparison of tissue oximeters on a liquid phantom with adjustable optical properties: an extension. *Biomed. Opt. Express* **9**, 86 (2018).

221. *IEC 80601-2-71:2015 - Medical electrical equipment — Part 2-71: Particular requirements for the basic safety and essential performance of functional Near-Infrared Spectroscopy (NIRS) equipment - https://www.iso.org/standard/61105.html*.

222. ISO 80601-2-85 - Medical electrical equipment — Part 2-85: Particular requirements for the basic safety and essential performance of cerebral tissue oximeter equipment. https://www.iso.org/standard/72442.html.

223. IEC - TC 62/SC 62D/JWG 5. https://www.iec.ch/dyn/www/f?p=103:14:5576978447608::::FSP_ORG_ID,FSP_LANG_ID:2492,25.

224. ISO - ISO/TC 121/SC 3 - Respiratory devices and related equipment used for patient care. https://www.iso.org/committee/52012.html.

225. Pogue, B. W. Perspective review of what is needed for molecular-specific fluorescence-guided surgery. *J. Biomed. Opt.* **23**, 1 (2018).

226. Alander, J. T. *et al.* A Review of Indocyanine Green Fluorescent Imaging in Surgery. *Int. J. Biomed. Imaging* **2012**, 1–26 (2012).

227. Nagaya, T., Nakamura, Y. A., Choyke, P. L. & Kobayashi, H. Fluorescence-guided surgery. *Frontiers in Oncology* vol. 7 (2017).

228. Roy, M., Kim, A., Dadani, F. & Wilson, B. C. Homogenized tissue phantoms for quantitative evaluation of subsurface fluorescence contrast. *J. Biomed. Opt.* **16**, 16013 (2011).

229. De Grand, A. M. *et al.* Tissue-like phantoms for near-infrared fluorescence imaging system assessment and the training of surgeons. **11**, 014007 (2006).

230. Samkoe, K. S., Bates, B. D., Tselepidakis, N. N., DSouza, A. V. & Gunn, J. R. Development and evaluation of a connective tissue phantom model for subsurface visualization of cancers requiring wide local excision. *J. Biomed. Opt.* **22**, 1 (2017).

231. Pleijhuis, R. *et al.* Tissue-simulating phantoms for assessing potential near-infrared fluorescence imaging applications in breast cancer surgery. *J. Vis. Exp.* e51776 (2014) doi:10.3791/51776.

232. van Willigen, D. M. *et al.* Multispectral fluorescence guided surgery; a feasibility study in a phantom using a clinical-grade laparoscopic camera system. *Am. J. Nucl. Med. Mol. Imaging* **7**, 138–147 (2017).

233. Würth, C., Hoffmann, K., Behnke, T., Ohnesorge, M. & Resch-Genger, U. Polymer- and glass-based fluorescence standards for the near infrared (NIR) spectral region. in *Journal of Fluorescence* vol. 21 953–961 (Springer, 2011).

234. DeRose, P. C., Smith, M. V., Mielenz, K. D., Blackburn, D. H. & Kramer, G. W. Characterization of Standard Reference Material 2941, uranyl-ion-doped glass, spectral correction standard for fluorescence. *J. Lumin.* **128**, 257–266 (2008).

235. DeRose, P. C., Smith, M. V., Mielenz, K. D., Blackburn, D. H. & Kramer, G. W. Characterization of Standard Reference Material 2940, Mn-ion-doped glass, spectral correction standard for fluorescence. *J. Lumin.* **129**, 349–355 (2009).

236. Liu, Y. *et al.* Biomimetic 3D-printed neurovascular phantoms for near-infrared fluorescence imaging. *Biomed. Opt. Express* **9**, 2810 (2018).

237. Koch, M., Symvoulidis, P. & Ntziachristos, V. Tackling standardization in fluorescence molecular imaging. *Nat. Photonics* doi:10.1038/s41566-018-0221-5.

238. Pogue, B. W. *et al.* Fluorescence-guided surgery and intervention - An AAPM emerging technology blue paper. *Med. Phys.* **45**, 2681–2688 (2018).

239. Kaufman, M. B. Pharmaceutical Approval Update. *P T* **42**, 673–683 (2017).

240. DSouza, A. V., Lin, H., Henderson, E. R., Samkoe, K. S. & Pogue, B. W. Review of fluorescence guided surgery systems: identification of key performance capabilities beyond indocyanine green imaging. *J. Biomed. Opt.* **21**, 080901 (2016).

241. Tummers, W. S. *et al.* Recommendations for reporting on emerging optical imaging agents to promote clinical approval. *Theranostics* vol. 8 5336–5347 (2018).

242. Hoogstins, C. *et al.* Setting Standards for Reporting and Quantification in Fluorescence-Guided Surgery. *Mol. Imaging Biol.* **21**, 11–18 (2019).

243. Pogue, B. W. *et al.* Update on AAPM task group 311: guidance for technical performance evaluation for fluorescence guided surgery systems (Conference Presentation). in *Molecular-Guided Surgery: Molecules, Devices, and Applications VI* (eds. Gibbs, S. L., Pogue, B. W. & Gioux, S.) vol. 11222 27 (SPIE, 2020).

244. Zhu, B., Rasmussen, J. C., Litorja, M. & Sevick-Muraca, E. M. Determining the Performance of Fluorescence Molecular Imaging Devices Using Traceable Working Standards with SI Units of Radiance. *IEEE Trans. Med. Imaging* **35**, 802–811 (2016).

245. Zhu, B., Kwon, S., Rasmussen, J. C., Litorja, M. & Sevick-Muraca, E. M. Comparison of NIR Versus SWIR Fluorescence Image Device Performance Using Working Standards Calibrated with SI Units. *IEEE Trans. Med. Imaging* **39**, 944–951 (2020).

246. Gorpas, D. *et al.* Multi-Parametric Standardization of Fluorescence Imaging Systems Based on a Composite Phantom. *IEEE Trans. Biomed. Eng.* **67**, 185–192 (2020).

247. Attia, A. B. E. *et al.* A review of clinical photoacoustic imaging: Current and future trends. *Photoacoustics* vol. 16 100144 (2019).

248. Beard, P. Biomedical photoacoustic imaging. *Interface Focus* **1**, 602–631 (2011).

249. Laufer, J., Zhang, E. & Beard, P. Evaluation of Absorbing Chromophores Used in Tissue Phantoms for Quantitative Photoacoustic Spectroscopy and Imaging. *IEEE J. Sel. Top. Quantum Electron.* **16**, 600–607 (2010).

250. Avigo, C. *et al.* Organosilicon phantom for photoacoustic imaging. *J. Biomed. Opt.* **20**, 046008 (2015).

251. Ratto, F. *et al.* Hybrid organosilicon/polyol phantom for photoacoustic imaging. *Biomed. Opt. Express* **10**, 3719–3730 (2019).

252. Gehrung, M., Bohndiek, S. E. & Brunker, J. Development of a blood oxygenation phantom for photoacoustic tomography combined with online pO2 detection and flow spectrometry. *J. Biomed. Opt.* **24**, 1 (2019).

253. Vogt, W. C. *et al.* Phantom-based image quality test methods for photoacoustic imaging systems. *J. Biomed. Opt.* **22**, 1 (2017).

254. FDA. Tissue-mimicking polymer test phantoms for optical-acoustic medical imaging | FDA. https://www.fda.gov/science-research/licensing-and-collaboration-opportunities/tissue-mimicking-polymer-test-phantoms-optical-acoustic-medical-

imaging.

255. Bohndiek, S. Addressing photoacoustics standards. *Nature Photonics* vol. 13 298 (2019).

256. Sun, J. Y. *et al.* Highly stretchable and tough hydrogels. *Nature* **489**, 133–136 (2012).

257. Sjoding, M. W., Dickson, R. P., Iwashyna, T. J., Gay, S. E. & Valley, T. S. Racial Bias in Pulse Oximetry Measurement. *N. Engl. J. Med.* **383**, 2477–2478 (2020).

258. Belykh, E. *et al.* Utilization of intraoperative confocal laser endomicroscopy in brain tumor surgery. *Journal of Neurosurgical Sciences* vol. 62 704–717 (2018).

259. Keenan, M. *et al.* Design and characterization of a combined OCT and wide field imaging falloposcope for ovarian cancer detection. *Biomed. Opt. Express* **8**, 124 (2017).

260. Masters, B. R. *et al.* Mitigating thermal mechanical damage potential during two-photon dermal imaging. *J. Biomed. Opt.* **9**, 1265 (2004).

261. Liang, W. *et al.* Increased illumination uniformity and reduced photodamage offered by the Lissajous scanning in fiber-optic two-photon endomicroscopy. *J. Biomed. Opt.* **17**, 021108 (2012).

262. *Qualification of Medical Device Development Tools | FDA*. https://www.fda.gov/regulatory-information/search-fda-guidance-documents/qualification-medical-device-development-tools (2017).

263. Clarke, G. D. *Overview of the ACR MRI Accreditation Phantom*.

264. IEC. *IEC 60601-2-37:2007 Particular requirements for the basic safety and essential performance of ultrasonic medical diagnostic and monitoring equipment*. https://webstore.iec.ch/publication/2652 (2007).

265. IEC TS 61206:1993 | IEC Webstore. https://webstore.iec.ch/publication/4909.

266. IEC 61685:2001 | IEC Webstore. https://webstore.iec.ch/publication/5721.

267. IEC TS 63081:2019 | IEC Webstore. https://webstore.iec.ch/publication/32282.

268. Bouchard, J.-P., Veilleux, I., Noiseux, I. & Mermut, O. Accurately characterized optical tissue phantoms: how, why and when? in *Optical Diagnostics and Sensing XI: Toward Point-of-Care Diagnostics; and Design and Performance Validation of Phantoms Used in Conjunction with Optical Measurement of Tissue III* vol. 7906 79060K (SPIE, 2011).

269. Aldrich, M. B. *et al.* Team Sciences and Core Resources within the NTR. in

*Translational Research in Biophotonics: Four National Cancer Institute Case Studies* 29–66 (Society of Photo-Optical Instrumentation Engineers, 2014). doi:10.1117/3.1002515.ch3.

270. Bouchard, J.-P. *et al.* Reference optical phantoms for diffuse optical spectroscopy Part 1 – Error analysis of a time resolved transmittance characterization method. *Opt. Express* **18**, 11495 (2010).

271. Heikka, T. *et al.* Testing a phantom eye under various signal-to-noise ratio conditions using eleven different OCT devices. *Biomed. Opt. Express* **11**, 1306 (2020).

272. EuropeanCommission. *Performance Assessement and Standardization in Biophotonics Workshop | Shaping Europe's digital future*. https://ec.europa.eu/digital-single-market/en/news/performance-assessement-and-standardization-biophotonics-workshop (2018).

273. EuropeanCommission. Standardisation and performance assessment in Biophotonics - the report | Shaping Europe's digital future. https://ec.europa.eu/digital-single-market/en/news/standardisation-and-performance-assessment-biophotonics-report (2019).

274. O'Connor, J. P. B. *et al.* Imaging biomarker roadmap for cancer studies. *Nat. Rev. Clin. Oncol.* **14**, 169–186 (2017).

275. Waterhouse, D. Translation of Optical Imaging Biomarkers: Opportunities and Challenges. *Nat. Biomed. Eng.* **3**, 339–353 (2019).

276. Blumenröther, E., Melchert, O., Wollweber, M. & Roth, B. Detection, numerical simulation and approximate inversion of optoacoustic signals generated in multi-layered PVA hydrogel based tissue phantoms. *Photoacoustics* **4**, 125–132 (2016).

277. Samarov, D. V. *et al.* Algorithm validation using multicolor phantoms. *Biomed. Opt. Express* **3**, 1300 (2012).

278. Manohar, S., Kharine, A., Hespen, J. van, Steenbergen, W. & Leeuwen, T. van. Photoacoustic mammography laboratory prototype: imaging of breast tissue phantoms. *J Biomed Opt* **9**, (2004).

279. Richards-Kortum, R. & Sevick-Muraca, E. Quantitative optical spectroscopy for tissue diagnosis. *Annu. Rev. Phys. Chem.* **47**, 555–606 (1996).

280. Lee, J. Y. K. *et al.* Review of clinical trials in intraoperative molecular imaging during cancer surgery. *J. Biomed. Opt.* **24**, 1 (2019).

281. Doyley, M. M. *et al.* Shear modulus estimation using parallelized partial volumetric reconstruction. *IEEE Trans. Med. Imaging* **23**, 1404–1416 (2004).

282. Jiang, S. Near-infrared breast tomography calibration with optoelastic tissue simulating phantoms. *J. Electron. Imaging* **12**, 613 (2003).

283. Hussain, A., Petersen, W., Staley, J., Hondebrink, E. & Steenbergen, W. Quantitative blood oxygen saturation imaging using combined photoacoustics and acousto-optics. *Opt. Lett.* **41**, 1720 (2016).

284. Pfefer, T. J., Chan, K. F., Hammer, D. X. & Welch, A. J. Dynamics of pulsed holmium:YAG laser photocoagulation of albumen. *Phys. Med. Biol.* **45**, 1099–1114 (2000).

285. Takegami, K. *et al.* Polyacrylamide gel containing egg white as new model for irradiation experiments using focused ultrasound. *Ultrasound Med. Biol.* **30**, 1419–1422 (2004).

286. Khokhlova, V. A. *et al.* Effects of nonlinear propagation, cavitation, and boiling in lesion formation by high intensity focused ultrasound in a gel phantom. *J. Acoust. Soc. Am.* **119**, 1834–1848 (2006).

287. Lafon, C. *et al.* Gel phantom for use in high-intensity focused ultrasound dosimetry. *Ultrasound Med. Biol.* **31**, 1383–1389 (2005).

288. Choi, M. J., Guntur, S. R., Lee, K. I. L., Paeng, D. G. & Coleman, A. A Tissue Mimicking Polyacrylamide Hydrogel Phantom for Visualizing Thermal Lesions Generated by High Intensity Focused Ultrasound. *Ultrasound Med. Biol.* **39**, 439–448 (2013).

289. Kennedy, G. T. *et al.* Solid tissue simulating phantoms having absorption at 970 nm for diffuse optics. *J. Biomed. Opt.* **22**, 076013 (2017).

290. Bykov, A. V., Popov, A. P., Priezzhev, A. V. & Myllyla, R. Multilayer tissue phantoms with embedded capillary system for OCT and DOCT imaging. in (eds. Leitgeb, R. A. & Bouma, B. E.) 80911R (2011). doi:10.1117/12.889923.

291. Xie, Y. *et al.* Soft optically-tuneable fluorescence phantoms based on gel wax and quantum dots: a tissue surrogate for fluorescence imaging validation. in *Molecular-Guided Surgery: Molecules, Devices, and Applications V* (eds. Pogue, B. W. & Gioux, S.) 10 (SPIE, 2019). doi:10.1117/12.2508348.

292. Cortela, G., Benech, N., Pereira, W. C. A. & Negreira, C. Characterization of acoustical properties of a phantom for soft tissues (PVCP and Graphite Powder) in the

range 20-45°C. in *Physics Procedia* vol. 70 179–182 (Elsevier, 2015).

293. De Carvalho, I. M. *et al.* Polyvinyl chloride plastisol breast phantoms for ultrasound imaging. *Ultrasonics* **70**, 98–106 (2016).

294. Li, W. *et al.* Polyvinyl chloride as a multimodal tissue-mimicking material with tuned mechanical and medical imaging properties. *Med. Phys.* **43**, 5577–5592 (2016).

295. Spinelli, L. *et al.* Calibration of scattering and absorption properties of a liquid diffusive medium at NIR wavelengths. Time-resolved method. *Opt. Express* **15**, 6589 (2007).

296. Madsen, E. L., Hobson, M. A., Shi, H., Varghese, T. & Frank, G. R. Stability of heterogeneous elastography phantoms made from oil dispersions in aqueous gels. *Ultrasound Med. Biol.* **32**, 261–270 (2006).

297. Chu, K. C. & Rutt, B. K. Polyvinyl alcohol cryogel: An ideal phantom material for MR studies of arterial flow and elasticity. *Magn. Reson. Med.* **37**, 314–319 (1997).

298. Jiang, S., Liu, S. & Feng, W. PVA hydrogel properties for biomedical application. *J. Mech. Behav. Biomed. Mater.* **4**, 1228–1233 (2011).

299. Yon, S. H. H. *et al.* Poly (Vinyl Alcohol) Hydrogels as Soft Contact Lens Material. *J. Biomater. Sci. Polym. Ed.* **5**, 397–406 (1994).

300. Martelli, F. *et al.* Phantoms for diffuse optical imaging based on totally absorbing objects, part 2: experimental implementation. *J. Biomed. Opt.* **19**, 076011 (2014).

## Figure Captions

**Figure 1: Tasks of phantoms along the translational pipeline.** Instrument- and application-specific tasks of phantoms are presented along the translational pipeline for optical imaging devices. Translational gap 1 refers to the step of transferring a research tool from a preclinical into a clinical research environment. Translational gap 2 refers to the step of integrating a tool from clinical research into clinical standard-of-care and routine patient-use. (pipeline broadly taken from[274,275]; SOPs = Standard operating procedures).

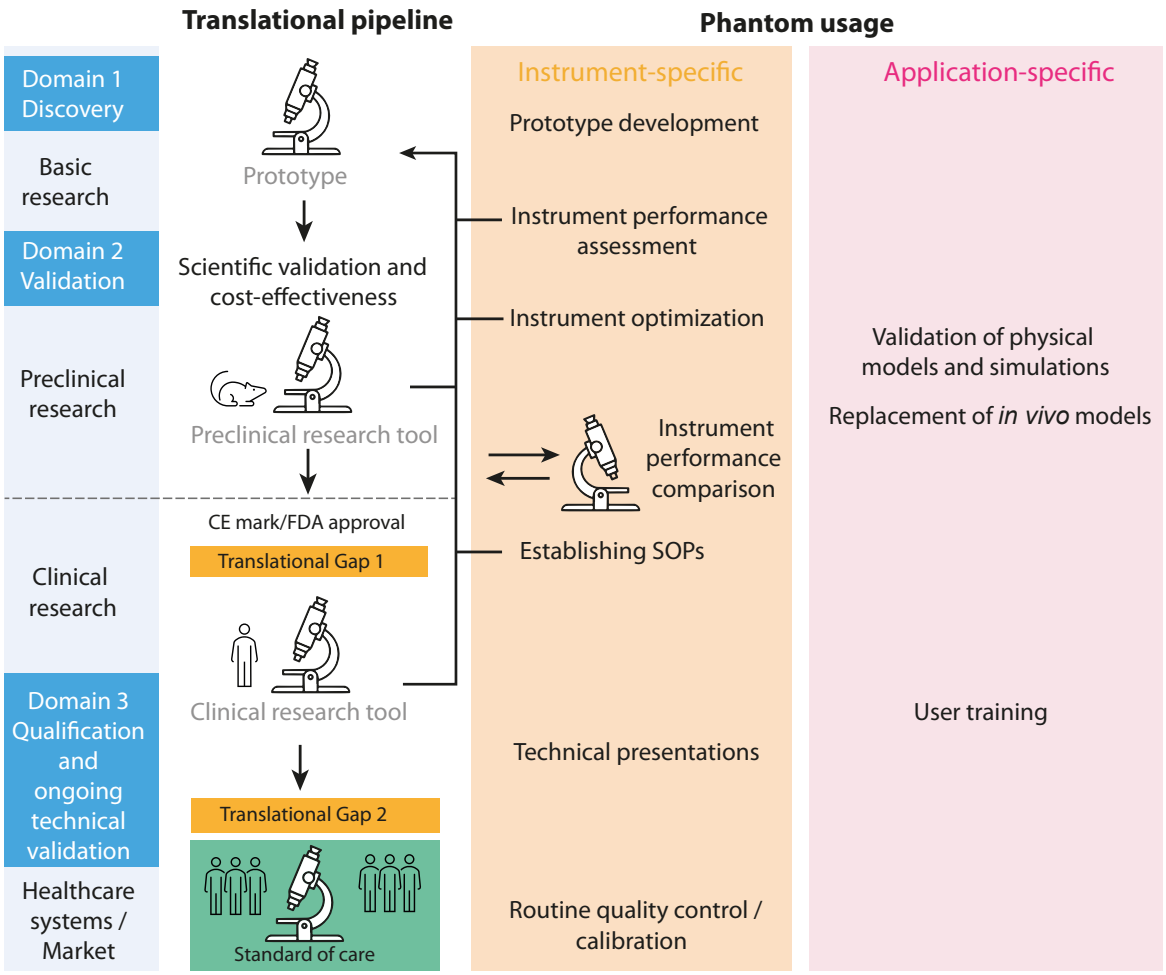

**Figure 2: Base requirements for a biophotonic phantom.** An ideal phantom material should possess the eight following characteristics: (1) Ability to provide tissue-like properties (including optical, acoustic, mechanical and thermoelastic properties); (2) Tunability of properties to mimic different tissue types; (3) Stability of all intrinsic properties over time and under different environmental conditions (including temporal, mechanical and photo-stability); (4) Architectural flexibility and ability to include absorbers/molecules of interest; (5) Simple and reproducible preparation; (6) Low maintenance (ease of storage and transport); (7) Safe to prepare and handle; (8) Readily available, low-cost ingredients and non-specialist fabrication equipment.

**Figure 3: Phantoms for diffuse optical imaging and spectroscopy: a,** Schematic showing the concept of time-domain functional near-infrared spectroscopy (TD-fNIRS): an ultra-short light pulse illuminates the tissue and the broadened and attenuated re-emitted pulse is detected after multiple scattering events. Photons with longer time of flight probe deeper tissue compartments. **b,** Liquid-solid phantom with black polyvinyl chloride (PVC) cylinders in a cell with aqueous Intralipid/ink suspension. Equivalence of the diffuse reflectance or transmittance for a totally absorbing inclusion and a moderately absorbing inclusion of larger volume was demonstrated[300] **c,** Contrast in the number of detected photons (relative change) for different depths of a 100 $mm^3$ black cylinder (equivalent to $\Delta\mu_a$=0.15 $cm^{-1}$ over 1 $cm^3$ for a background $\mu_s$'=10 $cm^{-1}$) as a function of depth. Increase of photon arrival times leads to higher contrast at greater depths. **d,** Solid-solid embodiment of the same phantom concept exploiting a rod with an embedded PVC cylinder which can be translated within an epoxy resin block with black toner and $TiO_2$ particles [120] **e,** Images of photon counts in different time windows (image titles) for the solid phantom scanned in transmittance geometry (without enclosing black plates) with a 50 $mm^3$ black inclusion ($\Delta\mu_a$=0.09 $cm^{-1}$ over 1 $cm^3$, $\mu_s$'=10 $cm^{-1}$) as obtained when testing imaging systems (e.g., optical mammographs). Spatial resolution is best for short photon arrival times (black: minimum, white: maximum photon count, scan area 20x20 $mm^2$) [120].

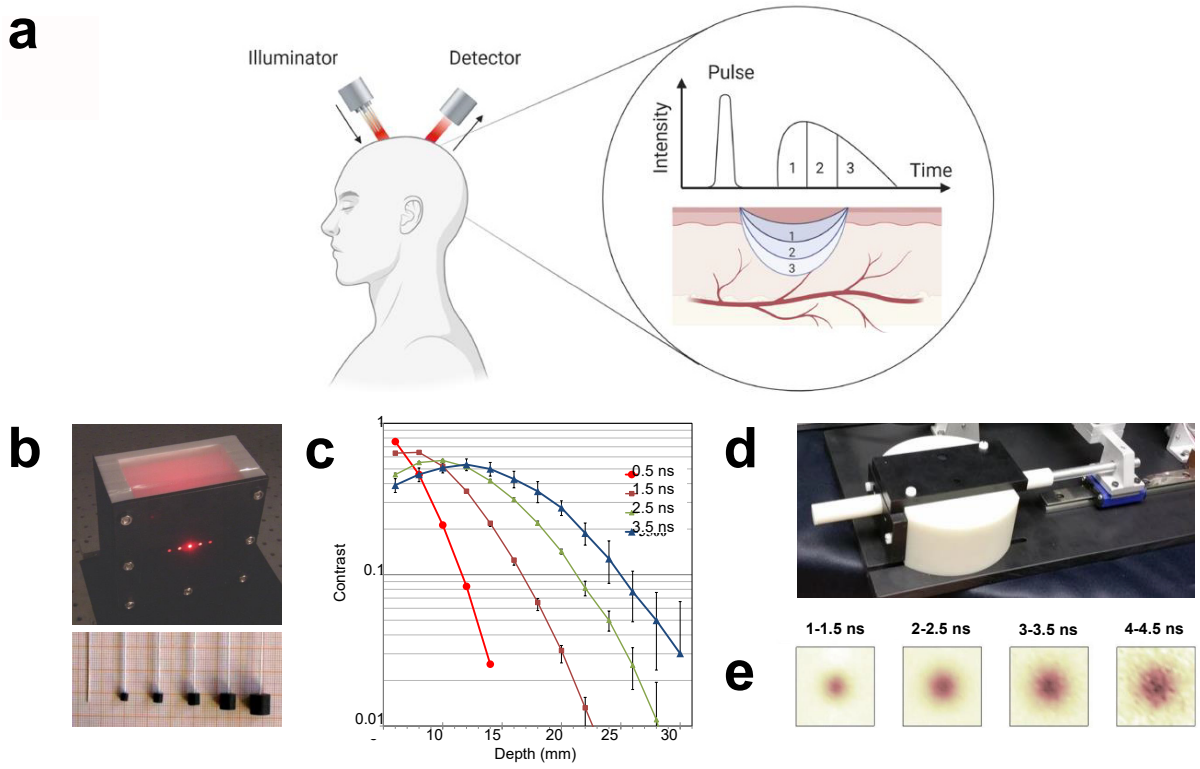

**Figure 3: Phantoms for fluorescence guided surgery. a,** Schematic showing the concept of fluorescence guided surgery (FGS): tissue during surgical intervention is illuminated by light, which is then absorbed by tissue components and exogenous contrast agents if present. Subsequently, fluorescent molecules in the contrast agent emit light of longer wavelength. A general Jablonski diagram (inset) shows the respective energetic transitions after optical excitation in the singlet state energy levels ($S_0$, $S_1$, $S_2$). **b,** Schematic explaining the function of the different parts of a polyurethane-based composite phantom proposed for fluorescence imaging in the visible range. Background absorption was set to ~2.2 $cm^{-1}$ by adding nigrosin dissolved in alcohol to the base material, while the reduced scattering coefficient was set to ~10 $cm^{-1}$ by adding 1 mg $g^{-1}$ $TiO_2$ particles. Different concentrations of organic quantum dots and hemin provide varying fluorescence and absorption properties, respectively. 'USAF chart' refers to the 1951 US Air Force (USAF) resolution test chart[27,237]. **c,** Colour photograph of the phantom, which has outer dimensions of 10 × 10 × 2.2 $cm^3$ [27,237]. **d,** Fluorescence image of the phantom acquired from a custom-built FGS instrument (EagleRay-V3)[27,237].

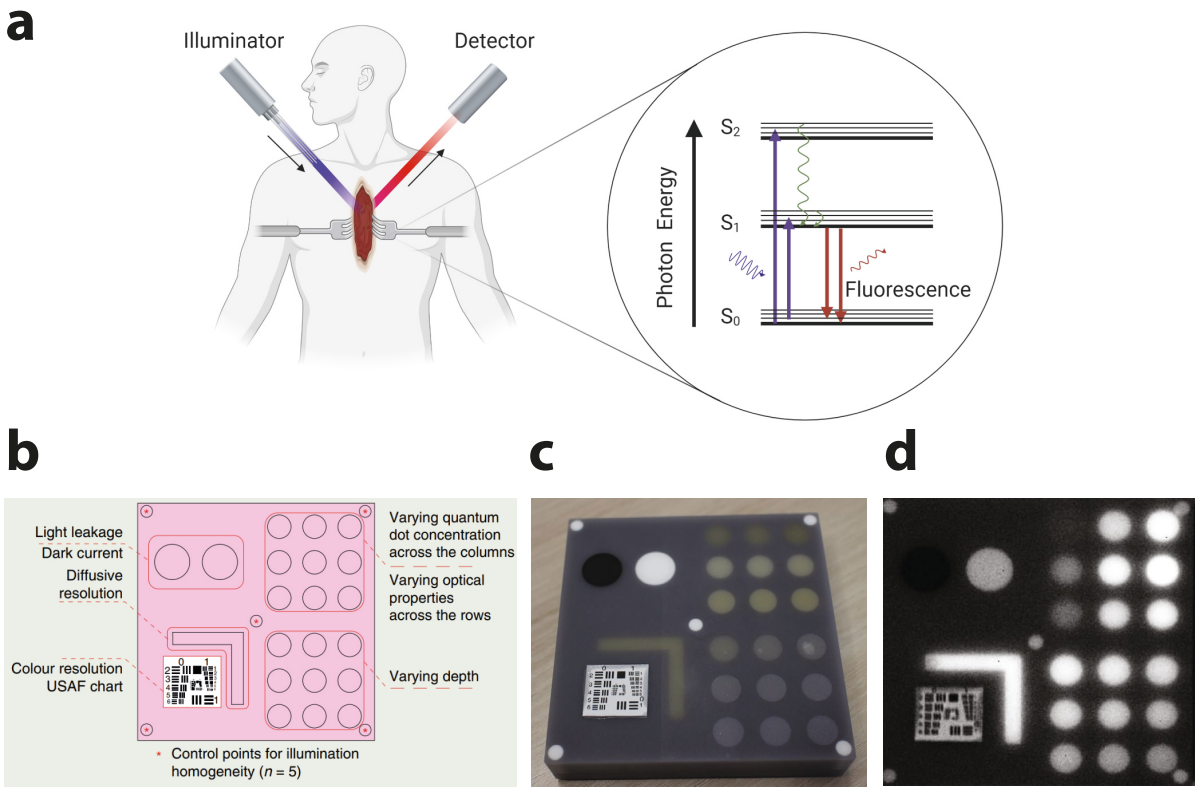

**Figure 5: Phantoms for photoacoustic imaging. a,** Schematic showing the concept of photoacoustic imaging (PAI): short light pulses are absorbed by endogenous chromophores within the tissue, leading to a temperature rise and pressure increase. The pressure rise generates broadband acoustic waves that are detected by ultrasound transducers. The amplitude and arrival time of the pressure wave provide information about the local energy propagation and position of the sample. **b,** Photoacoustic images of a coloured ink vessel phantom with four inclusions (green (top left), blue (top right), violet (bottom left), red (bottom right)) are shown as maximum intensity projections at different excitation wavelengths (550, 630, 725, 800 and 1210 nm). The field of view is 20 × 20 $mm^2$.[169] **c,** Photograph (top) and photoacoustic image (bottom) of a breast-shaped PVCP phantom[165].

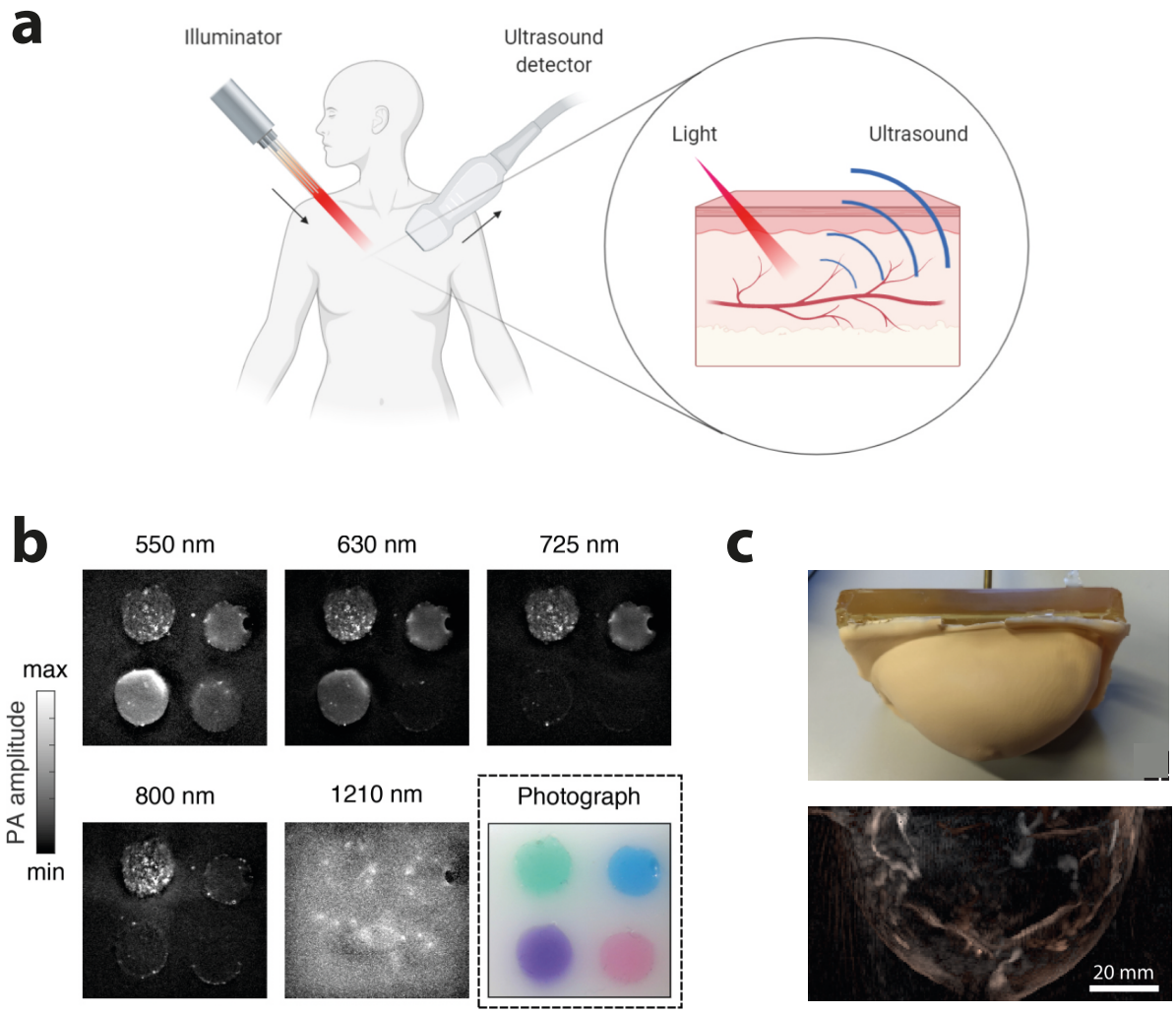

**Table 1: Common additives for tuning intrinsic properties in water-based phantom materials.**

| Function | | Additive |
|---|---|---|
| **Optical adjustment** | **Scattering $\mu_s'(\lambda)$** | Lipids (oil/fat[32,54–56], milk[57], intralipid[28–31,33] and similar[58]) |
| | | Microspheres[59,60] |
| | | Metal oxide suspensions (e.g., $Al_2O_3$ (1-10 µm)[37], $TiO_2$ (< 1µm)) |
| | **Absorption $\mu_a(\lambda)$** | Whole blood/erythrocytes/haemoglobin[56,59,65,68–71] |
| | | Melanin[276] |
| | | Pigment-based inks (e.g., India ink)[43,66,67,92] |
| | | Molecular dyes[61,62,277,278] |
| | **Fluorescence $\mu_{af}(\lambda)$, $I_e(\lambda)$, $\phi_{QY}$, $\tau$** | Biological Fluorophores (e.g., NADH, FAD, Collagen, Porphyrins)[279] |
| | | Quantum Dots[246] |
| | | Biomedical contrast agents (e.g., ICG, 800CW, Fluorescein)[133,280] |
| | | Laser dyes (e.g., IR125)[34] |
| **Acoustic adjustment** | **Speed of sound c(f)** | n-propanol[47,48] |
| | | Ethanol[64] |
| | | Glycerol[49] |
| | | Oil[50] |
| | | Formaldehyde[281] |
| | **Acoustic attenuation α(f)** | Graphite powder[47,48] |
| | | Evaporated milk[51] |
| | | $Al_2O_3$[37,49] |
| | **Acoustic backscattering $\mu_{bs}(f)$** | Glass beads[48,51–53] |
| | | Silicon carbide[49] |
| **Miscellaneous** | **Stability** | Benzalkonium chloride[49,96] |
| | | Thimerosal[51] |
| | | Formaldehyde[79] |
| | | EDTA |
| | | Penicilin[282], |
| | **Deoxygenation** | Yeast[65,71,219], sodium azide, sodium dithionite[180,252,283], glucose & glucose oxidase catalase, nitrogen gas |
| | **Oxygenation** | Oxygen gas, hydrogen peroxide[252] |
| | **Thermal damage** | Albumen[44,284] |
| | | Bovine Serum Albumin (BSA)[285–288] |
| | **Melting temperature** | Formaldehyde[79] |

**Table 2: Additives for tuning relevant acoustic and optical properties in non-water-based phantom materials proposed for biophotonic imaging.**

| | | Resin-based materials | Silicone | Polyvinyl chloride plastisol (PVCP) | Co-polymer in oil |
|---|---|---|---|---|---|
| **Optical adjustment** | **Scattering $\mu_s'(\lambda)$** | $TiO_2$[27,112]<br>$Al_2O_3$[117]<br>Glass or silica spheres[113]<br>Polystyrene microspheres[35,114,121] | $TiO_2$[40,138,139,141,145,147,149,152,289], $Al_2O_3$[92,135–137], $Ba_2SO_4$[151], polystyrene[135] silica[40,154] | $TiO_2$[159,160,164,290]<br>ZiO[38,39] | $TiO_2$[169] |
| | **Absorption $\mu_a(\lambda)$** | India Ink[121,124]<br>Dyes (eg. 900NP) [46,112,113,115,118,121,122]<br>Carbon powder[120,125] | India ink[147]<br>Carbon black[92]<br>Alcohol soluble Nigrosin[138]<br>Freeze dried bovine zinc phthalocyanine[139]<br>Yellow food dyes[139]<br>Infra-red dyes[139] | Black plastic colorant, Pigments [159–161]<br>Black ink[166]<br>Trypan blue[166]<br>Melanin powder[166] | Oil-based dyes[169] |
| | **Fluorescence $\mu_{af}(\lambda)$, $I_e(\lambda)$, $\phi_{QY}$, $\tau$** | Quantum Dots[27,122,132,244]<br>Biomedical contrast agents (e.g., ICG, 800CW, Fluorescein)[280]<br>Laser dyes (IR125) [133] | Biomedical contrast agents (e.g., ICG, Cy5, Fluorescein) [231,232] | - | Quantum dots[291] |
| **Acoustic adjustment** | **Speed of sound c(f)** | | Silicone oil,<br>Vaseline<br>Glycerin[158] | Hardener/softener[161]<br>Type of plasticizer[161] | Variation of polymer concentration (eg. SEBS, LDPE) glycerol[172–174] |
| | **Acoustic attenuation $\alpha(f)$** | | - | Glass microspheres[161],<br>Type of plasticizer[161];<br>Graphite powder[158,292,293] | Variation of polymer concentration (eg. SEBS, LDPE) glycerol[172–174] |
| | **Acoustic backscattering $\mu_{bs}(f)$** | - | - | Glass beads[165,294] | Glass spheres[170,173], Silica/graphite powder spheres[174], glycerol[172] |

**Table 3: Comparison of relevant properties of materials used for biophotonic phantoms** (TMM = Tissue-mimicking). Legend: green (++) = excellent performance; light green (+) = above-average performance; light red (-) = below-average performance; red (--) = poor performance in respective category.)

| | **TMM Properties** | | | **Handling** | | | **Fabrication** | | | | **References** |
|---|---|---|---|---|---|---|---|---|---|---|---|
| Material | Optical | Acoustic | Tuna-bility | Temporal Stability | Mecha-nical Stability | Storage/ Trans-port | Architec-tural Flexibility | Com-plexity | Safety | Biocom-patibility | |
| Aqueous suspension | ++ | - | + | - - | - - | - - | - | ++ | ++ | Yes | [43,295] |
| Agar/Gelatin | ++ | ++ | ++ | - | - | - | ++ | ++ | ++ | Yes | [47,48,51,52,79,80,83,296] |
| Polyacrylamide | ++ | ++ | ++ | - | + | - | ++ | + | - | Yes | [98] |
| PVA | ++ | ++ | ++ | + | + | - | ++ | - | ++ | Yes | [89,91,108,297–299] |
| Co-polymer in oil | ++ | + | + | ++ | ++ | ++ | ++ | + | ++ | No | [172–174] |
| PVCP | ++ | + | + | ++ | ++ | ++ | + | + | + | No | [90,97,161] |
| Silicone | ++ | - | + | ++ | ++ | ++ | ++ | + | ++ | No | [135,136,282] |
| Polyurethane | ++ | + | + | ++ | ++ | ++ | ++ | + | + | No | [27,46,112] |
| Polyester, Epoxy resin | ++ | - - | + | ++ | ++ | ++ | + | + | ++ | No | [35,114,115,124] |
| *Ex vivo* tissues | ++ | ++ | - - | - | ++ | - | - - | ++ | ++ | Yes | [5] |

1